

1 **Assessing the precision and accuracy of foraminifera elemental analysis at low ratios**

2

3

4 Wanyi Lu ^{1,2*}, Weifu Guo ^{2*}, Delia W. Oppo ²

5

6 ¹ State Key Laboratory of Marine Geology, Tongji University, Shanghai, China

7 ² Woods Hole Oceanographic Institution, Woods Hole MA, USA

8

9

10 Corresponding authors: luwanyi@tongji.edu.cn, wguo@whoi.edu

11

12

13

14 **Abstract**

15 The minor and trace element compositions of biogenic carbonates such as foraminifera are
16 important tools in paleoceanography research. However, most studies have focused primarily on
17 samples with element to calcium (El/Ca) ratios higher than the El/Ca range often found in benthic
18 foraminifera. Here, we systematically assess the precision and accuracy of foraminifera elemental
19 analysis across a wide range of El/Ca especially at relatively low ratios, using a method on a
20 Thermo Scientific iCAP Qc quadrupole Inductively Coupled Plasma Mass Spectrometer (ICP-
21 MS). We focus on two benthic foraminifera species, *Hoeglundina elegans* and *Cibicidoides*
22 *pachyderma*, and prepared a suite of solution standards based on their typical El/Ca ranges to
23 correct for signal drift and matrix effects during ICP-MS analysis and to determine analytical
24 precision. We observe comparable precisions with published studies at high El/Ca, and higher
25 relative standard deviations for each element at lower El/Ca, as expected from counting statistics.
26 The overall long-term analytical precision (2σ) of the *H. elegans*-like consistency standard
27 solutions was 6.5%, 4.6%, 5.0%, for Li/Ca, Mg/Ca, Mg/Li, and 6.4%, 10.0%, 4.2% for B/Ca,
28 Cd/Ca, Sr/Ca. The precision for *H. elegans*-like Mg/Li is equivalent to a temperature uncertainty
29 of 0.5 – 1.1 °C. Measurement precisions were also assessed based on three international standards
30 (one solution and two powder standards) and replicate measurements of *H. elegans* and *C.*
31 *pachyderma* samples. We provide file templates and program scripts that can be used to design
32 calibration and consistency standards, prepare run sequences, and convert the raw ICP-MS data
33 into molar ratios.

34 **Keywords:** ICP-MS, iCAP Qc, foraminifera, trace element, calcium

35 **Key points:**

36 • Higher relative standard deviations are reported at lower element/calcium values, as
37 expected from counting statistics.

38 • Consistency standards having similar ratios to the unknown samples provide an accurate
39 estimate of errors.

40 • For the *Hoeglundina elegans* Mg/Li - temperature proxy, analytical precision (2σ) is
41 equivalent to a temperature uncertainty of $0.5 - 1.1$ °C.

42

43 **1. Introduction**

44 Elemental ratios of foraminiferal shells are widely used to reconstruct past ocean conditions,
45 such as Mg/Ca or Mg/Li for seawater temperature (Bryan & Marchitto, 2008; Elderfield et al.,
46 2006; Rosenthal et al., 2006), Cd/Ca for nutrients (E. A. Boyle, 1992; Bryan & Marchitto, 2010),
47 B/Ca and Sr/Ca for carbonate ion concentrations (Rae et al., 2011; Rosenthal et al., 2006; Yu &
48 Elderfield, 2007), and the utility of many other elemental ratios to reconstruct past ocean
49 conditions are being explored. To robustly apply these proxies, accurate, high-precision elemental
50 measurements are needed.

51 However, most studies so far focus primarily on samples with relatively high element to calcium
52 ratios (El/Ca) such as Mg/Ca in planktonic foraminifera, and few studies have explicitly examined
53 the analytical precision at low El/Ca such as those often found in benthic foraminifera. For example,
54 for Li/Ca and Mg/Ca, published methods have yielded good precision at high El/Ca, e.g., 1 relative
55 standard deviation [RSD, calculated as $(SD/\text{average ratio} \times 100\%)$] generally $< 2\%$ for Li/Ca of 5 –
56 30 $\mu\text{mol/mol}$ and Mg/Ca of 0.4 – 5 mmol/mol. It is not always clear how these methods perform
57 at lower El/Ca. The possibility of poor precision at low El/Ca may be problematic, especially for
58 foraminifera species with significantly lower El/Ca. For example, Li/Ca, B/Ca, Mg/Ca, Cd/Ca,
59 and Sr/Ca in core-top samples for three commonly studied benthic foraminifera species
60 (*Hoeglundina elegans*, *Cibicidoides* spp., and *Uvigerina* spp.) vary by up to a factor of 10, e.g.,
61 Li/Ca of *Uvigerina* $>$ *Cibicidoides* $>$ *H. elegans*, and B/Ca of *Cibicidoides* $>$ *H. elegans* $>$
62 *Uvigerina*, reaching values as low as $\sim 1 \mu\text{mol/mol}$ for Li/Ca and $\sim 10 \mu\text{mol/mol}$ for B/Ca (Fig. 1).
63 The Mg/Ca and Cd/Ca are generally comparable among the three species, with Atlantic core-top
64 *H. elegans* showing the lowest Mg/Ca (median value of 1 mmol/mol) and Cd/Ca (median value of

65 0.02 $\mu\text{mol/mol}$). The Sr/Ca values are similar in *Cibicidoides* and *Uvigerina*, but the data spread
66 is larger in *H. elegans* (Fig. 1).

67 For paleo-reconstructions, especially quantitative reconstruction of seawater parameters such
68 as temperature, it is important to robustly constrain both the precision and accuracy of the
69 measurements. It is expected that samples with low molar ratios are more likely to be impacted by
70 measurement errors than those with higher ratios. For example, a relatively small inter-laboratory
71 offset in Li/Ca (+2.4%) and Mg/Ca (-2.6%) between Woods Hole Oceanographic Institution
72 (WHOI) and INSTAAR, University of Colorado can lead to temperature difference up to 3 °C
73 when applying the *H. elegans* Mg/Li - temperature proxy (Oppo et al., 2023), highlighting that
74 accurate measurements, not only good precision, are also needed.

75 Here we systematically assess the precision and accuracy of foraminiferal minor and trace
76 element analysis across a wide range of El/Ca ratios on a Thermo Scientific iCAP Qc quadrupole
77 Inductively Coupled Plasma Mass Spectrometer (ICP-MS), with a focus on relatively low ratios.
78 To achieve this goal, we design species-specific El/Ca calibration standards, matrix standards, and
79 consistency standards that closely match specific foraminiferal ratios. We also routinely measure
80 international standards treated as unknowns. In addition, we provide machine-specific
81 instrumentation parameters that can be used as references for the labs using or planning to use the
82 iCAP Qc quadrupole ICP-MS. We also provide a generalized method with a user guide and file
83 templates that begins with making a set of new standards and ends with obtaining El/Ca results (in
84 molar ratios, which are generally used for ocean property reconstructions).

85 **2. Methods**

86 **2.1. Instrumentation**

87 Element analyses were conducted on a Thermo iCAP Qc quadrupole ICP-MS interfaced to an
88 ESI SC4 DX autosampler at WHOI. During each analysis, sample solutions were pulled through
89 a peristaltic pump and nebulized at about 1 ml/min, and a quartz cyclonic spray chamber was used
90 to minimize memory effects due to sample washout. Nickel sampler and skimmer cones were used
91 with a quartz injector and torch. The instrument sensitivity was optimized at the beginning of each
92 day of analysis using the Thermo TuneB solution.

93 The iCAP uses two detection modes: standard (STD) mode, and kinetic energy discrimination
94 (KED) mode using helium gas in the collision cell. In the KED mode, unwanted polyatomic
95 interferences are filtered out based on the difference in collision cross-section sizes of the analyte
96 and polyatomic interferences, and lower masses have less kinetic energy and are less likely to
97 make it beyond the kinetic energy barrier. When both KED and STD modes are used for one
98 element, the raw counts per second (CPS) data are typically lower in KED mode than those in STD
99 mode. The El/Ca values are usually very similar in both modes. Table S1 lists the isotopes and
100 their modes used in this study.

101 The instrument detection limits (IDL) were determined from 16 replicates of the blank solution
102 (2% HNO₃) during the first analytical session, following the calculation method described in U.S.
103 EPA (2014). The IDL of the major and minor elements are Ca: 3.1 ppb; B: 0.05 ppb; Na: 17.77
104 ppb; Mg: 0.05 ppb; Al: 0.03 ppb; Ti: 0.06 ppb; Mn: 0.01 ppb; Fe: 0.16 ppb; Zn: 0.06 ppb; and Sr:
105 0.01 ppb. The IDL of four minor elements are in the level of ppt, Li: 0.15 ppt; Cd: 0.47 ppt; Ba:
106 0.44 ppt; and U: 0.01 ppt.

107 **2.2. Standards: Species-specific design**

108 Three distinct types of El/Ca standard solutions were prepared and employed in this study: 1)
109 calibration standards, which were used to calibrate the raw CPS data into molar ratios; 2) matrix
110 standards, which were used to correct for the matrix effects during the ICP-MS analysis, and 3)
111 consistency standards, which were used to monitor long-term data quality and to compare our
112 results to those of other laboratories. All standard solutions were prepared gravimetrically using
113 high purity Ca stock solution (10,000 ppm), and 14 minor or trace elements, which were each
114 added separately: lithium (Li), boron (B), magnesium (Mg), aluminum (Al), manganese (Mn), iron
115 (Fe), strontium (Sr), cadmium (Cd), barium (Ba), uranium (U), zinc (Zn), titanium (Ti), sodium
116 (Na), neodymium (Nd). Each stock standard solution has a volume of 250 mL containing ~1,000
117 ppm Ca and different amounts of minor and trace elements in a solvent of 2% HNO₃, and is freshly
118 diluted to a target Ca concentration for each analytical session. Note that the Ca stock solution
119 (10,000 ppm) should only contain minimum amounts of impurities that are much lower than in
120 foraminifera samples.

121 **2.2.1. Calibration standards**

122 We designed and prepared two separate sets of standards for each benthic species, based on the
123 El/Ca distribution in core-top samples (Fig. 1). Each standard set includes five calibration
124 standards (labeled as GLU in Fig. 2, file templates available in Table S1-S2), which were designed
125 to scatter throughout the El/Ca ranges among all core-top data of each species. The target Ca
126 concentrations in the analytical sessions range from 25 to 160 ppm in most labs (Cook et al., 2022;
127 Dai et al., 2023; Farmer et al., 2019; Stewart et al., 2021; Yu et al., 2005; Marchitto, 2006;
128 Rosenthal et al., 1999). We chose 100 ppm Ca as target concentration because we also evaluated
129 Cd (a nutrient tracer), whose concentrations are typically very low (on the order of < 0.10
130 $\mu\text{mol/mol}$ for Cd/Ca, Fig. 1). A higher target Ca concentration would result in higher CPS for Cd
131 (thus also smaller RSD).

132 **2.2.2. Matrix standards**

133 Because foraminiferal shells generally experience varying degrees of sample loss during the
134 cleaning processes (see section 2.3), the final sample solutions may have a wide range of Ca
135 concentrations, potentially causing matrix-related changes in instrumental mass bias (i.e.,
136 increased ion transmission with mass may cause deviations of measured ratios from true ratios).
137 Two approaches are typically used to overcome such matrix effects. One is through a pre-screening
138 of Ca concentrations by analyzing a small aliquot of sample solutions on an ICP-MS or ICP atomic
139 emission spectrometer (ICP-AES) or optical emission spectroscopy (ICP-OES), then diluting the
140 remainder to a near-constant Ca concentration for ICP-MS analyses (Yu et al., 2005). The other
141 one is by analyzing matrix-matched internal standards with a wide range of Ca concentrations,
142 fitting matrix curves to these data, and finally applying the corrections to the measured ratios of
143 the unknown samples (Marchitto, 2006; Rosenthal et al., 1999). The first approach is not feasible
144 on the iCAP at WHOI for most benthic foraminiferal samples because the sample uptake rate (1
145 ml/min) combined with the large number of elements we measure requires a minimum of 1 ml
146 solution. For relatively small samples, using an aliquot for pre-screening of Ca concentration may
147 lead to insufficient solution for iCAP analyses at 100 ppm Ca (our target matrix). We thus use the
148 second approach as it is relatively more efficient, assuming the matrix corrections work.

149 We designed and prepared three internal standards (designated as AFS for artificial foraminifera
150 solutions) for each benthic species, with a particular focus on Mg/Ca, Li/Ca, and Mg/Li, given the

151 implication of small differences in Mg/Li values for paleotemperature reconstructions. Similar to
152 the calibration standards, Mg/Li values of these AFS standards were selected to mimic those of the
153 benthic foraminifera analyzed with low, moderate, and high Mg/Li values (thus from different
154 temperature conditions) (Fig. 2). For each analytical session, we measure only one species of
155 benthic foraminifera and select two internal standards as matrix standards. These matrix standards
156 have El/Ca values close to those expected in the foraminiferal samples (e.g., AFS2 and AFS3 for
157 *H. elegans*, AFS4 and AFS5 for *C. pachyderma*). These AFS standards are then diluted to solutions
158 with Ca concentrations of 40, 60, 80, 100, 120, 150, 180, and 200 ppm, in order to produce matrix
159 correction curves for each session.

160 **2.2.3. Consistency standards**

161 To monitor the performance of our method, we use a third internal standard (AFS, see above)
162 as the consistency standard for each benthic species, e.g., AFS1 for *H. elegans*, and AFS6 for *C.*
163 *pachyderma* samples (Fig. 2). Note that AFS1 has lower elemental ratios than most core-top *H.*
164 *elegans* whereas AFS6 ratios are generally higher than core-top *C. pachyderma* (e.g., Fig. 2). The
165 selected internal consistency standard is diluted to different Ca concentrations (e.g., 60, 100, 150
166 ppm) and analyzed as an unknown for data quality control and to test the effectiveness of matrix
167 corrections. For elements of interests in this study (i.e., Li, Mg, B, Cd, and Sr), the ion
168 concentrations in the AFS1 solution at 100 ppm Ca, are much higher than the IDL, (e.g., >150
169 times for Li, >300 times for Mg, >15 times for B, >15 times for B, >25 times for Cd, and > 10,000
170 times for Sr).

171 In addition to the internal solution consistency standards, we use three international standards
172 (one solution and two powder standards) as consistency standards: RM8301-foram (solution,
173 National Institute of Standards and Technology, USA, Stewart et al., 2021), ECRM-752-1
174 (limestone powder, Bureau of Analyzed Samples Ltd, UK, Greaves et al., 2008), and BAM-RS3
175 (calcite powder, Bundesanstalt für Materialforschung und -prüfung, Germany, Greaves et al.,
176 2008)). Limestone ECRM-752-1 and calcite BAM-RS3 are used in every session for long-term
177 quality monitoring. RM8301-foram is only used in the sessions when we analyze *Cibicidoides*
178 samples, because its El/Ca values (e.g., Li/Ca, Mg/Ca, B/Ca, and Sr/Ca) are close to those in
179 *Cibicidoides* samples (Table 1).

180 **2.3. Foraminifera sample preparation**

181 Each of our measurements on the iCAP takes ~4 mins and requires ~1 ml solution to determine
182 14 El/Ca values. At our target Ca concentration of 100 ppm, ~240 µg of calcite is required for each
183 measurement, corresponding to approximately 300 to 400 µg of foraminiferal shells per sample
184 before cleaning. Foraminifera samples are weighed, then gently crushed to open chambers, and,
185 where sample size allows, split into two or more samples for replicate analysis. Samples are
186 cleaned following the full trace metal protocol (Boyle & Keigwin, 1985; Boyle & Rosenthal, 1996)
187 including clay removal (using methanol), reductive cleaning (using anhydrous hydrazine),
188 oxidative cleaning (using H₂O₂), and weak acid leaches (using 0.001 M HNO₃). After they are
189 cleaned, samples are dissolved with 100 µl of 2% HNO₃, sonicated for 15 mins, then centrifuged
190 for 10 mins at 10,000 rpm. Lastly, the samples are transferred to a set of new clean vials (already
191 containing 900 µl of 2% HNO₃) and mixed well using a vortex shaker before being analyzed on
192 the iCAP. The Ca concentration in the final 1 ml solution typically ranges between 40 and 150
193 ppm.

194 **2.4. Analytical sequence**

195 Our analytical session begins after daily tuning to optimize the instrument sensitivity, and
196 consists of three types of blocks: cone conditioning, matrix, and sample blocks (Fig. 3). The cone
197 conditioning consists of injecting one selected internal solution standard (in our example, AFS3 in
198 100 ppm Ca) for a few hours, in order to allow Ca deposition on cones to reach a maximum or
199 saturation state (thus resulting in stable signals), similar to the protocol reported in Yu et al. (2005).
200 A blank solution (2% HNO₃) is run every five AFS3 solutions for low background monitoring.
201 The cone conditioning typically takes 3 - 4 hours on the WHOI iCAP (Fig. S1).

202 After the cone is well-conditioned, the analytical session begins with two matrix blocks. Two
203 matrix blocks are placed in the beginning, middle, and the end of the sequence; and five sample
204 blocks are placed between the set of two matrix blocks. The structures of matrix and sample blocks
205 are similar, both starting with a blank solution (2% HNO₃), followed by sequences of two
206 calibration standards (GLU) bracketing every two unknown matrix standards or samples, ending
207 with a calibration standard (GLU4 in our example, file template in Table S4). For the matrix blocks,
208 two internal standards (AFS2 and AFS3 in our example) are analyzed across a range of Ca

209 concentrations that covers most foraminiferal samples, in order to produce matrix correction
210 curves for each session.

211 One or two consistency standards are randomly placed within each sample block for quality
212 control, including the internal solution standard (e.g., AFS1 for *H. elegans*, and AFS6 for *C.*
213 *pachyderma*, diluted to 60, 100, and 150 ppm Ca), powder limestone ECRM-752-1 and calcite
214 BAM-RS3 (both freshly weighed, dissolved, and diluted to 100 ppm Ca), and RM8301-foram
215 (freshly diluted to 100 ppm Ca, and only measured in the sessions analyzing *Cibicidoides* samples).
216 Each consistency standard is run two to three times during each session. All foraminifera samples,
217 matrix and consistency standards are run as unknowns in a randomized order during each session
218 to avoid machine memory effects.

219 **2.5. Data processing**

220 The data collected from the iCAP are processed in four steps using an in-house Matlab script,
221 to convert the raw CPS data offline into molar ratios:

222 (1) Blank correction: Our blank correction consists of two parts. First, we apply the
223 conventional blank correction, which aims to correct for potential impurities introduced by
224 the 2% HNO₃ used in standards, samples, and the rinse solution on iCAP. For this, we
225 estimate the expected blank values for each sample or standard through linear interpolation
226 of the measured values of adjacent blank solutions, and then subtract these estimated blank
227 values from the measured sample/standard values. Second, one additional blank correction,
228 applied only to calibration standards (GLU), corrects for impurities in the Ca stock solutions
229 used to prepare these standards. Specifically, we subtract the measured values of standard
230 GLU0 (prepared from only the Ca stock solution) from the measured values of all other
231 calibration standards (GLU).

232 (2) Standard calibration: For all samples, we convert the measured CPS for each element
233 (except Ca) to its respective molar abundance based on standard calibration lines which
234 depict the relationship between the measured CPS for each element and its respective
235 gravimetrically-determined molar abundance within the standard solutions. Since samples
236 are embedded in repeated sequences of standards, multiple standard calibration lines are
237 typically generated for each sample, with each calibration line consisting of one complete

238 set of standards (e.g., from GLU0 to GLU4) that encloses the sample in the analytical
239 sequence (Fig. 3C-D). The molar abundances derived from all calibration lines are then
240 averaged to derive the final corrected values for each element in the sample. Similarly, we
241 determine the Ca abundance in each sample by comparing the measured Ca CPS in the
242 sample, the average Ca CPS measured in each calibration standard, and the gravimetrically-
243 determined Ca molar abundances of the standard solutions.

244 (3) Matrix correction: Matrix effects are quantified by fitting the correlation between the
245 measured El/Ca in the two matrix standards and their respective Ca abundances (2nd-order
246 polynomial). These equations are then applied to the measured sample El/Ca to derive the
247 final El/Ca for each sample or consistency standard (treated as unknowns).

249 **3. Results and Discussion**

250 **3.1. Signal drift and correction**

251 Similar to other types of ICP-MS (Marchitto, 2006; Yu et al., 2005), the sensitivity of most
252 elements measured on the iCAP typically decreases throughout the session, due to salt deposition
253 on the sampling cones. Signal drift varies among elements and from run to run. Among the five
254 elements of interest (Li/Ca, Mg/Ca, B/Ca, Cd/Ca, and Sr/Ca), the signal corrections typically vary
255 between 0 and 10 % during a 24-hr session (Fig. S2-3). The signal drift is usually gradual and
256 effectively corrected by our calibration standards (Fig. S2-3). As an example, we selected
257 consistency standards AFS2 and AFS3 (all at 100 ppm Ca) measured at the beginning, middle, and
258 end of one analytical session, and normalized their El/Ca values to their respective first
259 measurements before (CPS/CPS) and after (molar ratios) the standard corrections (Fig. 4). Their
260 El/Ca values after the standard corrections are typically within $\pm 5\%$ and do not show consistent
261 trends with time, confirming the signal drifts have been effectively corrected.

262 **3.2. Matrix effects and correction**

263 Matrix effects also vary among elements and analytical sessions, typically ranging from ~ 5 to
264 10% for Li/Ca, Mg/Ca, and Cd/Ca, and as high as 20 % for B/Ca and Sr/Ca over the range of 40-
265 200 ppm measured Ca concentrations (relative to El/Ca values measured at 100 ppm Ca) (Fig. S4).
266 During most sessions, negative matrix effects were observed in B/Ca and Cd/Ca, and a positive
267 matrix effect was observed in Sr/Ca, whereas the signs of the trends varied for Li/Ca and Mg/Ca.

268 Since the fitted matrix effect equations vary among analytical sessions, each session requires its
269 own set of matrix corrections. The overall magnitudes of matrix effects we observed (mostly \pm 5-
270 10% in all analytical sessions) are comparable to those observed on other types of ICP-MS
271 (Marchitto, 2006; Rosenthal et al., 1999; Yu et al., 2005), although the trends for each El/Ca differ
272 among these machines.

273 Fig. 5 shows an example of fitted matrix curves of five El/Ca in one analytical session. In this
274 session, both matrix solutions (AFS2 and AFS3) with high Ca (expected concentrations of 150,
275 180, 200 ppm based on pipette dilution) yielded lower measured Ca concentrations (140, 160, and
276 180 ppm, respectively), indicating signal suppression, possibly due to salt precipitation on the
277 cones during the analysis. However, signal suppression seems to have occurred to a similar extent
278 for Li/Ca, Mg/Ca, B/Ca, and Cd/Ca, thus leading to overall relatively small El/Ca matrix effects
279 (within \pm 5% in this session) across the 150 - 200 ppm range of true Ca concentrations. Relatively
280 larger variations of Li/Ca, B/Ca and Cd/Ca are found in the solutions of 40 ppm Ca, possibly due
281 to their lower counting statistics as fewer atoms would be introduced into the plasma and ionized
282 (also see section 3.3).

283 To evaluate the effectiveness of our matrix corrections, we use two datasets: (1) internal
284 consistency standard solutions (AFS1 and AFS6); and (2) a large set of foraminifera sample
285 replicates (a total of 18 *H. elegans* and 24 *C. pachyderma* samples from several cores in the
286 Atlantic Ocean, with 3-7 measurements for each sample). Both the internal consistency standard
287 solutions and foraminifera samples were measured across a wide range of Ca concentrations and
288 treated as unknowns in the analyses. We first normalize each measured El/Ca value to the
289 respective average value of its replicates [unit in %, calculated as (measured/average*100-100)],
290 then group the data by their measured Ca concentrations in 20 ppm bins (Fig. 6). We observe no
291 consistent trends in the normalized El/Ca across the whole range of Ca concentrations, suggesting
292 our matrix correction is overall effective. The range of normalized El/Ca values is generally larger
293 in foraminifera samples (\sim \pm 10%) compared to those in the AFS1 and AFS6 solutions (\sim \pm 5%), as
294 expected from larger heterogeneity within the natural foraminifera samples than lab-prepared
295 standard solutions. The normalized El/Ca variations are relatively larger in *H. elegans* than in *C. pachyderma*
296 samples, and similarly, the *H. elegans*-like AFS1 solutions show larger normalized

297 El/Ca variations than those in *Cibicidoides*-like AFS6. We infer these differences are amplified in
298 *H. elegans* and AFS1 because of their relatively lower average El/Ca (also see section 3.3).

299 For AFS1 solutions, the mean El/Ca values at different Ca concentrations are within error of
300 each other, although the variations are generally larger at 60 ppm Ca than at higher Ca, particularly
301 for Li/Ca, potentially due to larger uncertainty at lower counting statistics (Li/Ca of ~1.3
302 $\mu\text{mol/mol}$). To further examine this issue, we checked the AFS1 data in all analytical sessions,
303 comparing the normalized data of raw CPS/CPS to the ratios after calibration correction and after
304 matrix corrections (Fig. S5). We find that for Li/Ca, Mg/Ca, and Cd/Ca, neither the calibration
305 correction nor matrix corrections seem to increase or reduce the scatter, suggesting the El/Ca
306 variations mainly derive from the raw data noise. For B/Ca and Sr/Ca, matrix corrections
307 effectively correct for El/Ca variations induced by different Ca concentrations in the solution (Fig.
308 S5). Furthermore, because we used AFS2 and AFS3 (Li/Ca of ~3.3 and 4.3 $\mu\text{mol/mol}$, respectively)
309 as matrix standards to correct AFS1 which has much lower Li/Ca (1.31 $\mu\text{mol/mol}$, or 40% of
310 AFS2), it is possible that using a matrix standard having Li/Ca closer to the expected mean value
311 of the unknowns would improve the outcome. For example, using AFS4 and AFS5 (Li/Ca of ~12.2
312 and 16.4 $\mu\text{mol/mol}$, respectively) as matrix standards to correct AFS6 (Li/Ca of ~10.2 $\mu\text{mol/mol}$,
313 or ~80% of AFS4) run at different Ca concentrations yields better results, with fewer systematic
314 differences in mean value and standard deviations (Fig. 6), perhaps because of the higher elemental
315 ratios and the greater proximity (as a percent) of AFS6 to the matrix standards used.

316 **3.3. Precision and accuracy**

317 The long-term precision and accuracy of this method were determined using nine consistency
318 standards, including six internal solutions (AFS1-AFS6), one external solution (RM8301-foram),
319 and two external powder materials (limestone ECRM-752-1, and calcite BAM-RS3), over a period
320 of 15 months from May 2022 to August 2023 (Table 1). We note that AFS2-AFS5 solutions at 100
321 ppm Ca were treated as unknowns during data processing, thus they are also used for long-term
322 data quality control. The El/Ca 2SD in the two solid standards are generally similar to those
323 reported in both AFS and RM8301-foram solutions. Across the full range of the El/Ca measured
324 in both internal and external standards, the average long-term precisions (2σ) are Li/Ca = 0.21
325 $\mu\text{mol/mol}$ (4.8%), Mg/Ca = 0.06 mmol/mol (3.8%), B/Ca = 3.8 $\mu\text{mol/mol}$ (4.4%, for B/Ca > 5

326 $\mu\text{mol/mol}$), $\text{Cd/Ca} = 0.006 \mu\text{mol/mol}$ (10.0%, for $\text{Cd/Ca} < 0.15 \mu\text{mol/mol}$), and $\text{Sr/Ca} = 0.03$
327 mmol/mol (4.2%) (Table 1). The average 2RSD are within 5% for Na/Ca , Mn/Ca , Ba/Ca , and U/Ca ;
328 10-20% for Ti/Ca and Fe/Ca ; higher for Al/Ca (33%) and Zn/Ca (37%) (supplementary tables).

329 The accuracy of most El/Ca are within 5%, except for Al/Ca and Fe/Ca . Because we typically
330 use Al/Ca and Fe/Ca ratios to assess potential sample contamination (e.g., $> 100 \mu\text{mol/mol}$
331 suggests suspected contamination), the semi-quantitative measured values are sufficient for most
332 paleoceanography research purposes. For the five elements of interest, the measured mean values
333 closely follow the 1:1 line with reference values (Fig. 7). Notably, the internal standards generally
334 show smaller deviations from the 1:1 line (mostly $\pm 2\%$) than external standards (mostly $\pm 2\text{-}5\%$).
335 The reference El/Ca values of internal standards are most likely true values as they were
336 gravimetrically determined. In contrast, the reference El/Ca values of external standards (calcite
337 BAM-RS3, limestone ECRM-752-1, and solution RM8301-foram) are the mean values reported
338 by other labs, and the larger deviation from the 1:1 line may reflect a contribution from inter-lab
339 differences.

340 The relative standard deviations of El/Ca are expected to positively correlate with the $1/\sqrt{[\text{El/Ca}]}$ if the measurement noise follows counting statistics and the $\text{El/Ca} \ll 1$ (similar to
341 what has been theoretically derived for stable isotope ratio measurements, (Hayes, 1983)). Our
342 precisions across a wide range of El/Ca generally follow this expectation, yielding higher RSD
343 values at lower El/Ca (Fig. 8). For example, for Li/Ca and Mg/Ca , their 2RSD values increase
344 from 2.4% to 5.0% and from 3.0% to 8.2%, respectively, with a factor of ~ 2 decrease in the El/Ca .
345 Together, these yield precisions of 2.3% to 7.7% (2RSD) for Mg/Li , with AFS1 and AFS6 (our
346 two internal consistency standards at varying Ca concentrations) showing 7.7% and 2.3% 2RSD
347 respectively (Fig. 8). At the high El/Ca end, our precisions are comparable to other labs, which use
348 either an iCAP (Dai et al., 2023; Ford et al., 2016) or a different type of ICP-MS (Ford et al., 2016;
349 Marchitto, 2006; Yu et al., 2005).

351 **3.4. Implications for the *H. elegans* Mg/Li thermometry**

352 The precisions we report at low El/Ca have implications for *H. elegans* paleothermometry.
353 Note that Mg/Li of *C. pachyderma* should not be used to estimate temperature, because dividing

354 Mg/Ca by Li/Ca in *C. pachyderma* does not fully correct for the influence of carbonate saturation
355 state on Mg/Ca (Oppo et al., 2023). Using the *H. elegans* Mg/Li-temperature calibration equation
356 of Oppo et al. (2023), the 7.7% 2RSD of Mg/Li in AFS1 (± 0.016 mol/mmol) is equivalent to a
357 temperature error of ± 1.1 °C (at 1.5 °C). For AFS2, the 4.0% 2RSD (± 0.007 mol/mmol) is
358 equivalent to ± 0.5 °C (at 0.3 °C), and for AFS3, the 3.3% 2RSD (± 0.010 mol/mmol) is equivalent
359 to a temperature error of ± 0.7 °C (at 8.7 °C).

360 Importantly, the temperature precision is not only a function of temperature or Mg/Li itself, but
361 related to the specific Mg/Ca and Li/Ca of the sample, which can vary considerably for a single
362 temperature (Marchitto et al., 2018) (Fig. 8). For example, although the Mg/Li of AFS1 and AFS2
363 were both designed to mimic foraminifera calcifying in cold water, their elemental compositions,
364 and associated measurement precisions, are different. The very low Li/Ca (1.3 μ mol/mol) and
365 Mg/Ca (0.26 mmol/mol) in AFS1 occur in core-top *H. elegans* from the deep subpolar North
366 Atlantic where temperatures are ~ 1.1 °C. The higher Li/Ca (4.4 μ mol/mol) and Mg/Ca (0.8
367 mmol/mol) in AFS2 correspond to *H. elegans* found in the glacial Atlantic sediments, where
368 estimated temperatures are ~ 0.5 °C (Valley et al., 2019; Umling et al., 2019; Oppo et al., 2023).
369 Thus, the temperature error is larger for AFS1 than for AFS2, despite the similarity in their Mg/Li
370 values. This finding underscores the need to match the El/Ca of consistency standards to those of
371 the unknown for accurate estimation of measurement precisions.

372 **4. Summary**

373 We assess the precision and accuracy of foraminiferal minor and trace element measurements
374 on an iCAP across a range of El/Ca values, using a species-specific method. In particular, the
375 internal consistency solution standards are designed to match the expected elemental ratios of real
376 samples being measured, and are run with a range of Ca concentrations similar to foraminifera
377 samples. Based on the results from these consistency solution standards, we estimate the precision
378 for *H. elegans* Mg/Li measurements range from 3.3 to 7.7 % (0.007 to 0.016 mol/mmol), which is
379 equivalent to an uncertainty in Mg/Li-derived temperatures of 0.5 – 1.1 °C. Overall, the precision
380 of foraminiferal element analysis depends on the actual El/Ca values in the samples, which can
381 vary depending on oceanic regions, temperature, or time frame. The 2RSDs are higher at low El/Ca
382 values as expected from counting statistics. Due to the heterogeneity of foraminifera samples, the

383 average errors on replicate samples of foraminifera are ~8.0 %, larger than on internal consistency
384 solution standards, and are thus associated with larger Mg/Li-derived temperature uncertainties.

385

386 **Acknowledgments**

387 We thank N. Umling and G. Swarr for establishing the initial method on the iCAP at WHOI.
388 We also thank G. Swarr for technical support on the iCAP and many helpful discussions on method
389 improvements. We thank S. Wang, K. Pietro, and D. Belobokova for lab assistance. This work was
390 funded by NSF OCE-1811305 (to D.W.O. and W.G.), OCE-2114579 (to D.W.O) and the WHOI
391 Investment in Science Fund. W.L. also acknowledges financial support from the Fundamental
392 Research Funds for the Central Universities in China and Shanghai Pilot Program for Basic
393 Research.

394

395 **Open Research**

396 The file templates for standard preparation, session sequence, and standard dilution, and the
397 Matlab scripts to process the raw ICP-MS data are available in the supplementary materials and
398 Zenodo (citation link will be available upon acceptance).

399 **Author contributions**

400 Conceptualization: W. Guo, D.W. Oppo, W. Lu
401 Data curation: W. Lu, W. Guo
402 Formal analysis: W. Lu, W. Guo, D.W. Oppo
403 Funding acquisition: D.W. Oppo, W. Guo, W. Lu
404 Investigation: W. Lu, W. Guo, D.W. Oppo
405 Methodology: W. Lu, W. Guo, D.W. Oppo
406 Project administration: D.W. Oppo
407 Resources: D.W. Oppo
408 Software: W. Guo, W. Lu
409 Supervision: W. Guo, D.W. Oppo
410 Validation: W. Lu, W. Guo, D.W. Oppo
411 Writing – original draft: W. Lu
412 Writing – review & editing: W. Lu, W. Guo, D.W. Oppo

413 Table 1. Long-term precision and accuracy for five selected El/Ca determined from internal and external consistency standards, and
 414 average precision of foraminifera samples based on 3-7 replicates (n = 18 for *H. elegans*, n = 24 for *C. pachyderma*).

Standard/samples	n	LiCa_mean µmol/mol	LiCa_2sd µmol/mol	LiCa_2rsd %	Expected µmol/mol	Reference value µmol/mol	Accuracy %	MgCa_mean mmol/mol	MgCa_2sd mmol/mol	MgCa_2rsd %	Expected mmol/mol	Reference value mmol/mol	Accuracy %	MgLi_mean mol/mmol	MgLi_2sd mol/mol	MgLi_2rsd %	Expected mol/mol	Reference value mol/mol	Accuracy %
AFS1	66	1.31	0.06	5.0	1.31		-0.4	0.26	0.02	8.2	0.26		2.7	0.20	0.016	7.7	0.20		3.2
AFS2	58	4.36	0.12	2.8	4.33		0.7	0.80	0.03	3.8	0.81		-0.4	0.18	0.007	4.0	0.19		-1.1
AFS3	24	3.32	0.11	3.4	3.30		0.3	1.02	0.03	3.0	1.02		0.6	0.31	0.010	3.3	0.31		0.2
AFS4	15	16.40	0.39	2.4	16.39		0.1	1.52	0.05	3.3	1.51		0.9	0.09	0.003	3.6	0.09		0.8
AFS5	15	12.35	0.43	3.5	12.24		0.9	2.84	0.08	2.9	2.81		1.1	0.23	0.006	2.5	0.23		0.2
AFS6	33	10.32	0.28	2.7	10.24		0.7	3.24	0.10	3.1	3.20		1.0	0.31	0.007	2.3	0.31		0.3
BAM-RS3	17	1.23	0.15	11.9		1.22		0.75	0.03	3.4		0.79		0.61	0.072	11.8		0.65	
ECRM-752-1	29	1.57	0.15	9.6		1.39		3.57	0.13	3.8		3.75		2.28	0.217	9.5		2.70	
RM8301_foram	16	8.81	0.22	2.5		9.01		2.52	0.07	2.9		2.62		0.29	0.004	1.6		0.29	
<i>H. elegans</i>		0.41	12.2					0.14	16.9					0.020	8.0				
<i>C. pachyderma</i>		0.39	3.2					0.09	8.6					0.008	8.9				

Standard/samples	n	BCa_mean µmol/mol	BCa_2sd µmol/mol	BCa_2rsd %	Expected µmol/mol	Reference value µmol/mol	Accuracy %	SrCa_mean mmol/mol	SrCa_2sd mmol/mol	SrCa_2rsd %	Expected mmol/mol	Reference value mmol/mol	Accuracy %	CdCa_mean µmol/mol	CdCa_2sd µmol/mol	CdCa_2rsd %	Expected µmol/mol	Reference value µmol/mol	Accuracy %
AFS1	66	32.3	2.6	8.2	30.0		7.4	0.51	0.02	4.3	0.50		1.5	0.047	0.004	9.3	0.046		2.2
AFS2	58	41.7	3.0	7.2	40.4		3.1	1.01	0.03	3.3	1.00		0.9	0.067	0.004	5.3	0.066		1.1
AFS3	24	52.1	2.0	3.9	49.8		4.5	2.02	0.05	2.6	2.02		0.1	0.080	0.006	7.5	0.077		3.6
AFS4	15	203.0	6.0	3.0	200.8		1.1	1.31	0.03	2.2	1.32		-0.2	0.077	0.004	5.5	0.076		2.1
AFS5	15	183.7	5.3	2.9	181.4		1.3	1.51	0.04	2.9	1.50		0.7	0.048	0.005	11.3	0.046		6.0
AFS6	33	142.1	4.3	3.0	139.9		1.6	1.02	0.04	3.4	1.01		1.1	0.127	0.008	6.5	0.126		0.5
BAM-RS3	17	4.7	4.7	101.0				0.19	0.02	7.7		0.18		0.038	0.009	24.8		0.033	
ECRM-752-1	29	3.9	2.4	60.5				0.18	0.01	8.0		0.18		0.584	0.097	16.6		0.544	
RM8301_foram	16	138.7	3.4	2.4	138.9			1.30	0.04	3.4		1.34		0.570	0.024	4.3		0.580	
<i>H. elegans</i>		8.4	17.2					0.16	10.2					0.006	15.7				

<i>C. pachyderma</i>	5.5	3.7	0.04	3.2	0.007	10.7
----------------------	-----	-----	------	-----	-------	------

415

416 Notes:

417 1. Because the AFS and GLU standards were prepared from the same bottle of high purity Ca stock solution, we calculated the
 418 expected values of AFS solutions by first determining the impurities of Ca stock solutions (using the GLU calibration standard
 419 curves), and then accounting for the impurities in the gravimetric values of AFS solutions.

420 2. The reference values of BAM-RS3 and ECRM-752-1 refer to those reported from INSTAAR, University of Colorado (Greaves
 421 et al., 2008), and those of RM8301-foram refer to the average values reported from several laboratories (Stewart et al., 2021).

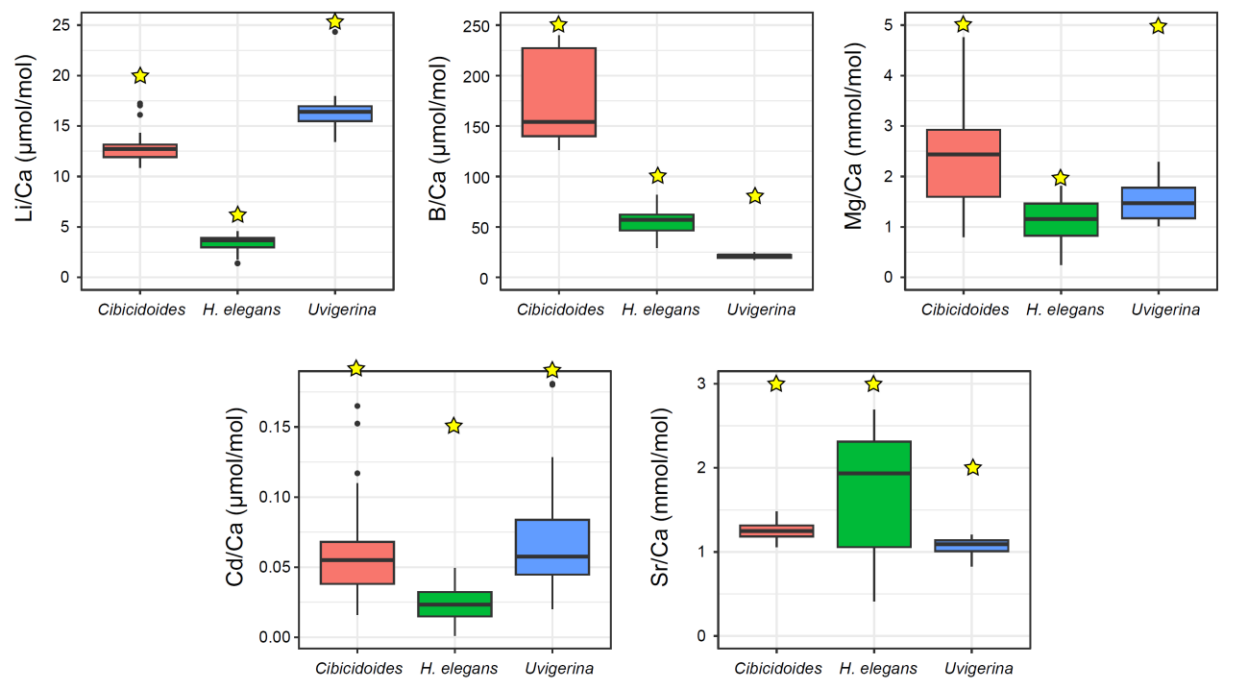
422 3. Accuracy = (measured mean - expected)/expected*100%.

423 4. The B/Ca 2RSD of BAM-RS3 and ECRM-752-1 are relatively high due to their low average B/Ca, and the Cd/Ca in ECRM-
 424 752-1 and RM8301-foram are outside of the calibration standard range, thus these values are excluded from the calculation of
 425 average long-term precisions.

426

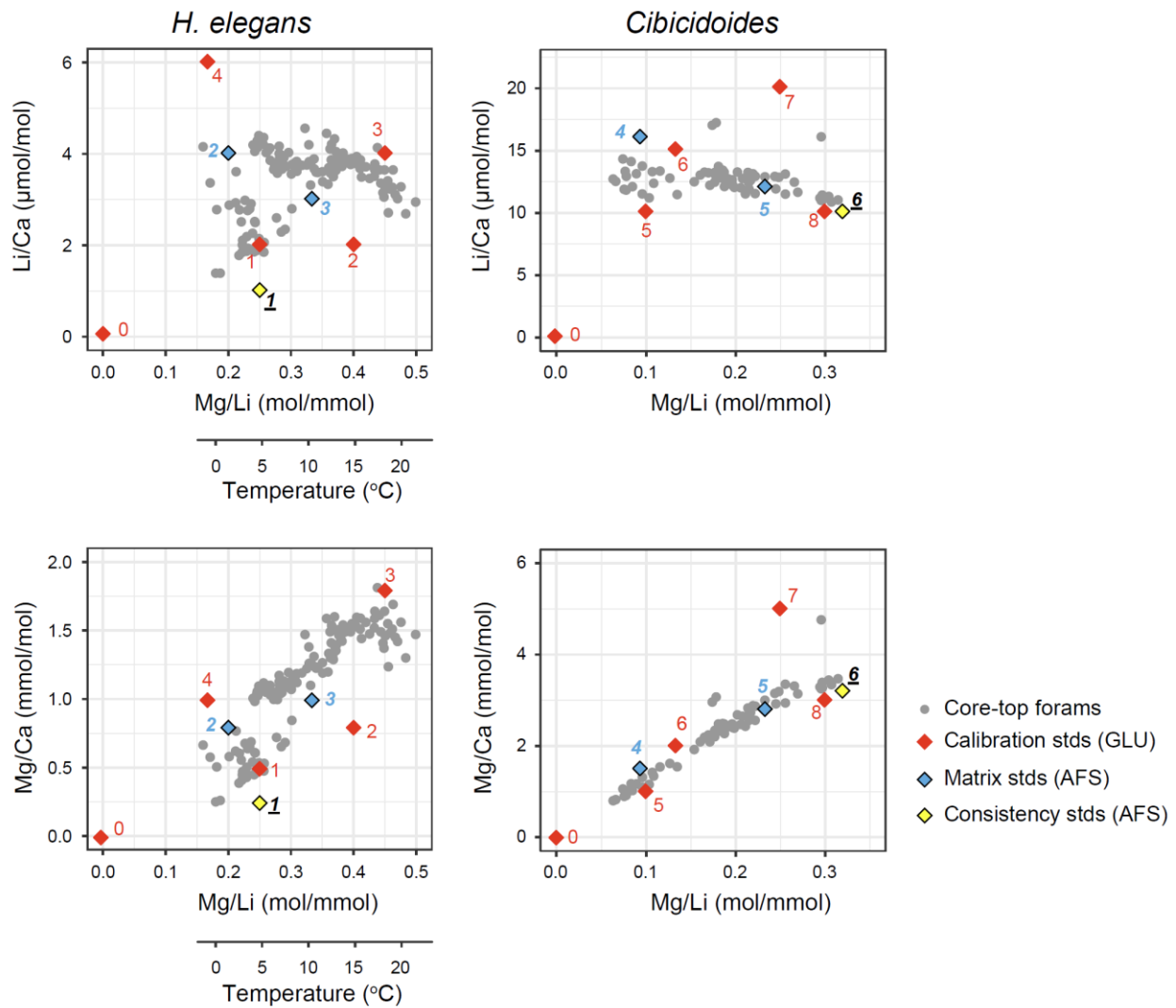
427 **Figures**

428



429

430 **Fig. 1.** Boxplot of five selected El/Ca in three benthic foraminifera species from core-top samples.
 431 The Li/Ca, B/Ca, Mg/Ca, and Cd/Ca data are only from three Atlantic regions (Bryan & Marchitto,
 432 2008, 2010; Oppo et al., 2023; Umling et al., 2019), but they are comparable to those from global
 433 core-tops (Elderfield et al., 2006; Rae et al., 2011; Stirpe et al., 2021; Tisserand et al., 2013; Yu &
 434 Elderfield, 2007); Sr/Ca data are from global core-tops (Oppo et al., 2023; Yu et al., 2014). The
 435 El/Ca data distributions are used to guide the design of calibration and internal consistency
 436 standards. Yellow stars mark the maximum El/Ca in each calibration standard set.

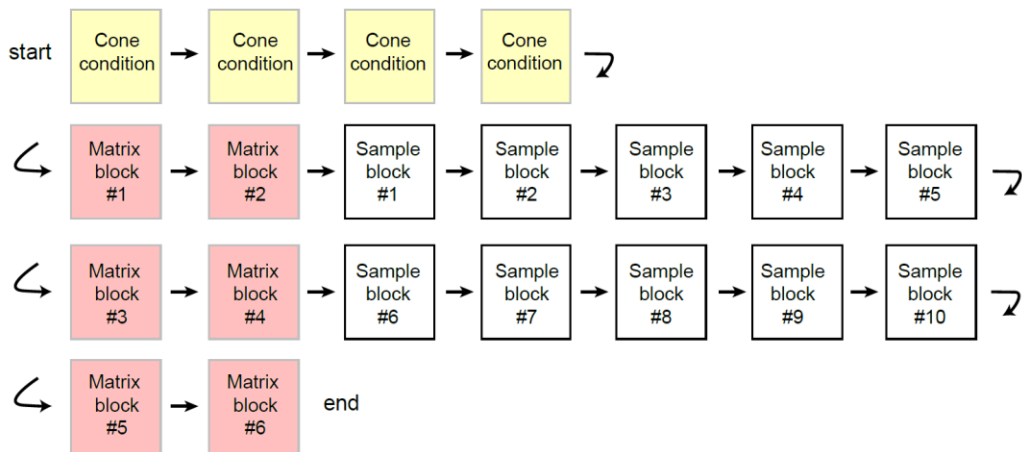


437

438 **Fig. 2.** Cross-plot of Mg/Li vs. Li/Ca and Mg/Ca in two benthic foraminifera species from core-
 439 top samples and their corresponding standard sets prepared at WHOI. The calibration standards
 440 (GLU, label numbers with red fonts) are designed to scatter at four corners of all core-top data,
 441 whereas the matrix and consistency standards (AFS) are designed to match low, moderate, high
 442 Mg/Li (thus temperature) endmembers. The *H. elegans* Mg/Li - temperature conversions use the
 443 equation from Oppo et al. (2023).

444

A) Session structure



B) Cone conditioning

Blank (2% HNO ₃)
AFS3_100ppmCa
Blank (2% HNO ₃)
AFS3_100ppmCa
Blank (2% HNO ₃)
AFS3_100ppmCa

C) Matrix block

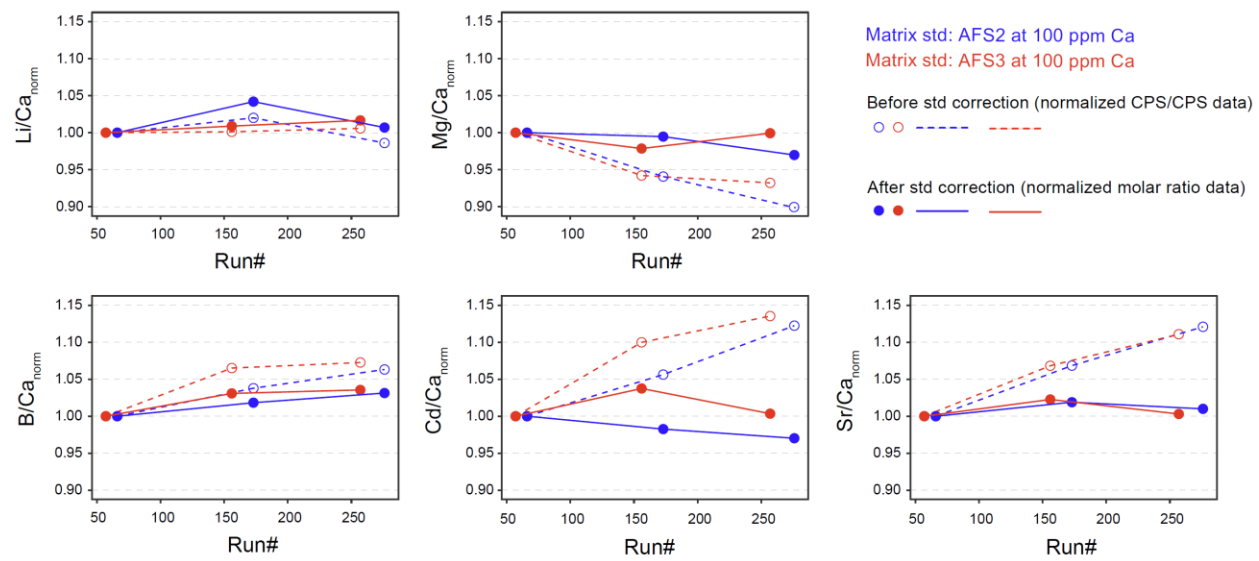
Blank (2% HNO ₃)
GLU0_Std
Matrix 1
Matrix 2
GLU1_Std
Matrix 3
Matrix 4
GLU2_Std
Matrix 5
Matrix 6
GLU3_Std
Matrix 7
Matrix 8
GLU4_Std

D) Sample block

Blank (2% HNO ₃)
GLU0_Std
Sample 1
Sample 2
GLU1_Std
Sample 3
Sample 4
GLU2_Std
Sample 5
Sample 6
GLU3_Std
Sample 7
Sample 8
GLU4_Std

447 **Fig. 3.** Schematic illustration of a full session sequence used to run *H. elegans* samples. After cone
 448 conditioning, the matrix blocks are placed in the beginning, middle, and end of the session. One
 449 or two consistency standards (e.g., AFS, and international standards) are placed within each sample
 450 block for quality control. Note that all matrix standards, consistency standards, and unknown
 451 samples are run in randomized order to avoid memory effects.

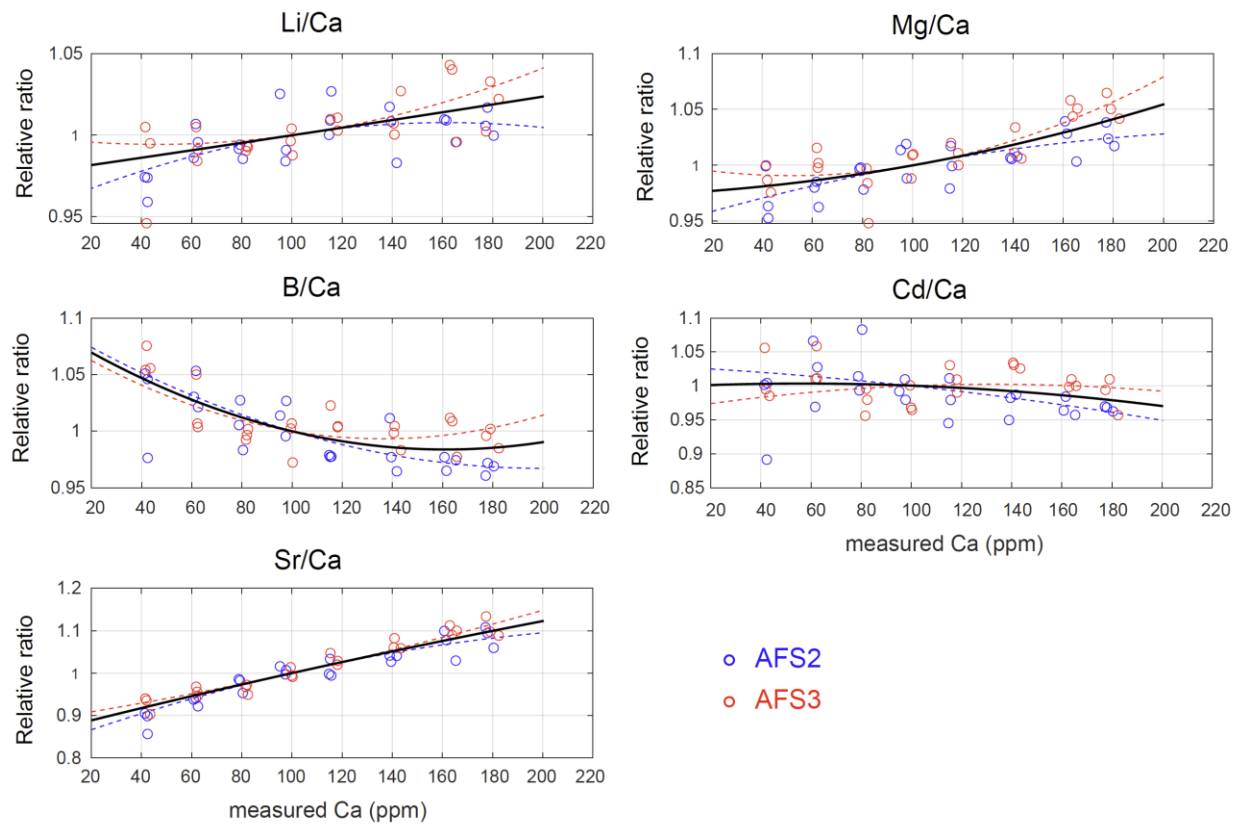
453



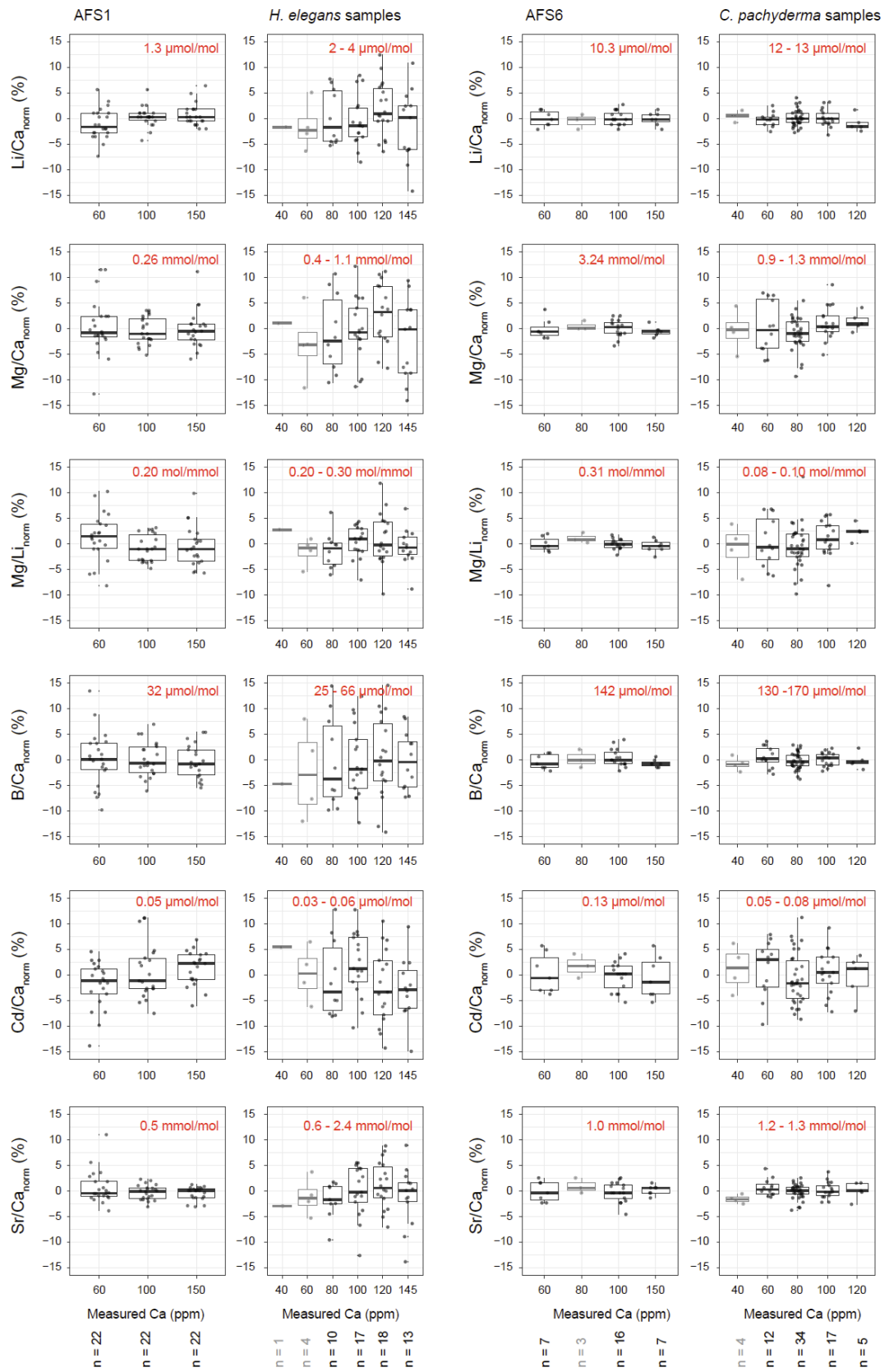
454

455 **Fig. 4.** Effect of signal drift correction in a representative session, based on Li/Ca, Mg/Ca, B/Ca,
456 Cd/Ca, and Sr/Ca of two internal standard solutions - AFS2 and AFS3 (matrix standards, all at 100
457 ppm Ca concentration).

458

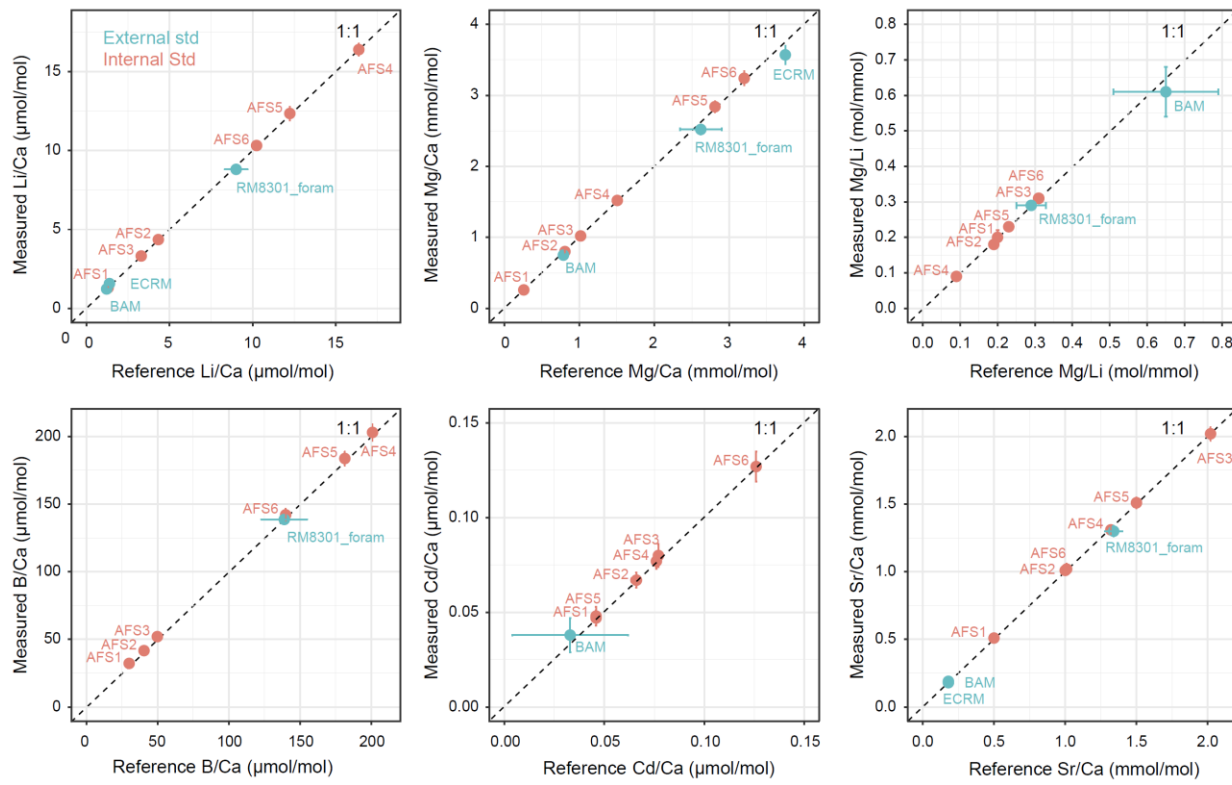


462 **Fig. 5.** Matrix effects and curves determined in a representative session, for Li/Ca, Mg/Ca, B/Ca,
 463 Cd/Ca, and Sr/Ca ratios over measured Ca concentrations of 40 to 180 ppm. The blue and red
 464 dashed lines denote the fitting for the AFS2 and AFS3 matrix standards, respectively, and show
 465 generally minor differences. The black line which fits all AFS data is used in the final matrix
 466 correction. Note that at high Ca concentrations, there are differences between measured (140,
 467 160, 180 ppm) and expected values (150, 180, 200 ppm based on pipette dilution), indicating
 468 signal suppression. However, the signal suppression occurs for all other elements (except for Sr)
 469 to a similar extent, leading to minor drifts in El/Ca values. Note varying range of vertical axes.
 470

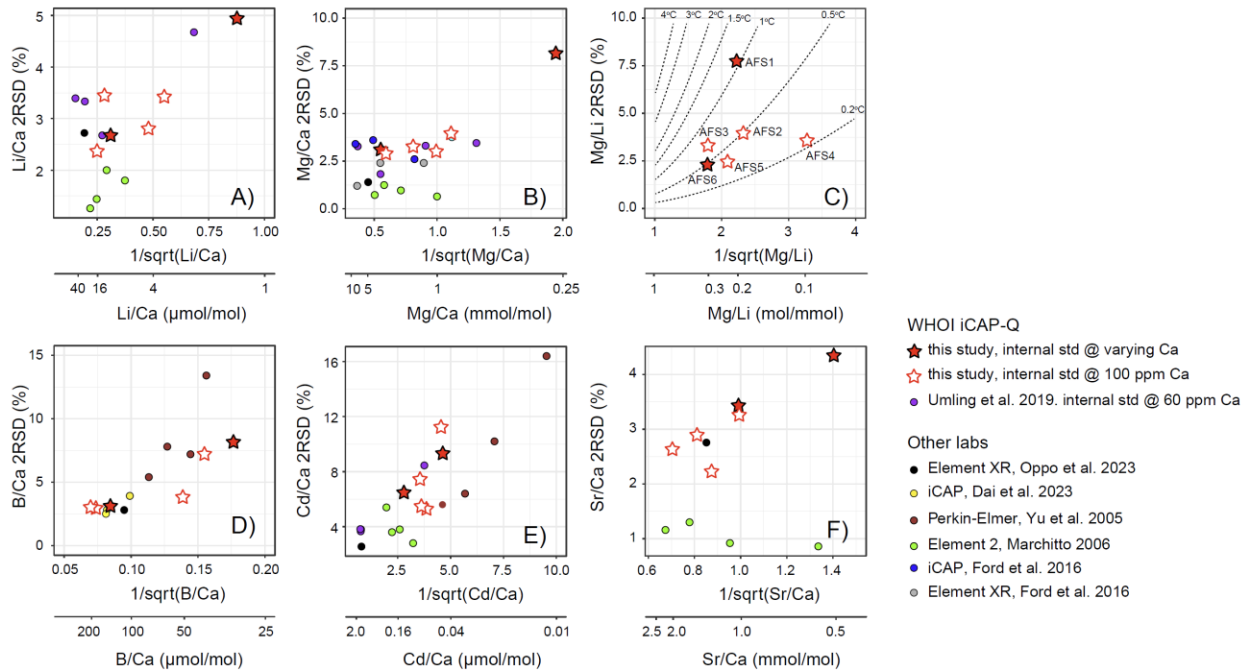


472 **Fig. 6.** Matrix and drift corrected El/Ca ratios of internal solution consistency standards (AFS1
473 and AFS6) and benthic foraminifera sample replicates (3-7 measurements for each sample),
474 normalized relative to the respective averages and binned by the measured Ca concentrations (20
475 ppm bin size). Normalized El/Ca at different measured Ca concentrations overlap, confirming the
476 effectiveness of the matrix corrections. Red fonts show the average El/Ca of AFS1 or AFS6, or the
477 El/Ca range of the sample replicates. Data with small sampling size ($n < 5$) are shown in grey.
478 Note that the last bin in *H. elegans* is centered at 145 ppm Ca. Random jitters are added to the x-
479 axis positions to avoid overlapping points.

480



483 **Fig. 7.** Comparisons of the measured mean EI/Ca values of internal and external standards vs. their
484 corresponding reference values (Table 1). The reference EI/Ca for internal standards are
485 determined from known gravimetric values corrected for impurities from the Ca stock solutions,
486 whereas the reference EI/Ca for external standards BAM-RS3 and ECRM-752-1 refer to those
487 reported from INSTAAR, University of Colorado (Greaves et al., 2008), and those of RM8301-
488 foram refer to the average values reported from several laboratories (Stewart et al., 2021). Note
489 that the Cd/Ca in ECRM-752-1 and RM8301-foram are outside of the calibration standard range,
490 thus these values are not plotted here (but listed in Table 1).



493

494 **Fig. 8.** Precisions of El/Ca measurements across a range of El/Ca ratios (this study, Table 1) and
495 their comparison with published studies (Dai et al., 2023; Ford et al., 2016; Marchitto, 2006; Oppo
496 et al., 2023; Umling et al., 2019; Yu et al., 2005). This compilation only includes lab-prepared
497 solution consistency standards. Note varying range of vertical axes. The contour lines in panel C)
498 denote the uncertainties in Mg/Li-derived temperatures (labels) at the corresponding Mg/Li values
499 and 2RSD precisions, showing that the same Mg/Li 2RSD implies different temperature precision
500 at different Mg/Li values (and hence temperatures). Note that the Mg/Li – temperature conversion
501 is only applicable on *H. elegans* (Oppo et al., 2023).

502

503

504

505 **References**

506 Boyle, E., & Rosenthal, Y. (1996). Chemical Hydrography of the South Atlantic During the Last Glacial
507 Maximum: Cd vs. $\delta^{13}\text{C}$. In *The South Atlantic*. https://doi.org/10.1007/978-3-642-80353-6_23

508 Boyle, E. A. (1992). Cadmium and $\delta^{13}\text{C}$ paleochemical ocean distributions during the stage 2 glacial
509 maximum. *Annual Review of Earth and Planetary Sciences*. Vol. 20.
510 <https://doi.org/10.1146/annurev.earth.20.1.245>

511 Boyle, E. A., & Keigwin, L. D. (1985). Comparison of Atlantic and Pacific paleochemical records for the
512 last 215,000 years: changes in deep ocean circulation and chemical inventories. *Earth and Planetary
513 Science Letters*, 76(1–2). [https://doi.org/10.1016/0012-821X\(85\)90154-2](https://doi.org/10.1016/0012-821X(85)90154-2)

514 Bryan, S. P., & Marchitto, T. M. (2008). Mg/Ca-temperature proxy in benthic foraminifera: New
515 calibrations from the Florida Straits and a hypothesis regarding Mg/Li. *Paleoceanography*, 23(2).
516 <https://doi.org/10.1029/2007PA001553>

517 Bryan, S. P., & Marchitto, T. M. (2010). Testing the utility of paleonutrient proxies Cd/Ca and Zn/Ca in
518 benthic foraminifera from thermocline waters. *Geochemistry, Geophysics, Geosystems*, 11(1).
519 <https://doi.org/10.1029/2009gc002780>

520 Cook, M. K., Dial, A. R., & Hendy, I. L. (2022). Iodine stability as a function of pH and its implications
521 for simultaneous multi-element ICP-MS analysis of marine carbonates for paleoenvironmental
522 reconstructions. *Marine Chemistry*, 245. <https://doi.org/10.1016/j.marchem.2022.104148>

523 Dai, Y., Yu, J., & Ji, X. (2023). Prolonged deep-ocean carbonate chemistry recovery after the Paleocene-
524 Eocene Thermal Maximum. *Earth and Planetary Science Letters*, 620.
525 <https://doi.org/10.1016/j.epsl.2023.118353>

526 Elderfield, H., Yu, J., Anand, P., Kiefer, T., & Nyland, B. (2006). Calibrations for benthic foraminiferal
527 Mg/Ca paleothermometry and the carbonate ion hypothesis. *Earth and Planetary Science Letters*,
528 250(3–4). <https://doi.org/10.1016/j.epsl.2006.07.041>

529 Farmer, J. R., Hönisch, B., Haynes, L. L., Kroon, D., Jung, S., Ford, H. L., et al. (2019). Deep Atlantic
530 Ocean carbon storage and the rise of 100,000-year glacial cycles. *Nature Geoscience*, 12(5).
531 <https://doi.org/10.1038/s41561-019-0334-6>

532 Ford, H. L., Sosdian, S. M., Rosenthal, Y., & Raymo, M. E. (2016). Gradual and abrupt changes during
533 the Mid-Pleistocene Transition. *Quaternary Science Reviews*, 148.
534 <https://doi.org/10.1016/j.quascirev.2016.07.005>

535 Greaves, M., Caillon, N., Rebaubier, H., Bartoli, G., Bohaty, S., Cacho, I., et al. (2008). Interlaboratory
536 comparison study of calibration standards for foraminiferal Mg/Ca thermometry. *Geochemistry,
537 Geophysics, Geosystems*, 9(8). <https://doi.org/10.1029/2008GC001974>

538 Hayes, J. M. (1983). Practice and principles of isotopic measurements in organic geochemistry. In W. G.
539 Meinschein (Ed.), *Organic geochemistry of contemporaneous and ancient sediments* (pp. 5.1–5.31).

540 Marchitto, T. M. (2006). Precise multielemental ratios in small foraminiferal samples determined by
541 sector field ICP-MS. *Geochemistry, Geophysics, Geosystems*, 7(5).
542 <https://doi.org/10.1029/2005GC001018>

543 Marchitto, T. M., Bryan, S. P., Doss, W., McCulloch, M. T., & Montagna, P. (2018). A simple
544 biomineralization model to explain Li, Mg, and Sr incorporation into aragonitic foraminifera and
545 corals. *Earth and Planetary Science Letters*, 481, 20–29. <https://doi.org/10.1016/j.epsl.2017.10.022>

546 Oppo, D. W., Lu, W., Huang, K.-F., Umling, N. E., Guo, W., Yu, J., et al. (2023). Deglacial temperature
547 and carbonate saturation state variability in the tropical Atlantic at Antarctic Intermediate Water
548 Depths. *Paleoceanography and Paleoclimatology*, 38, e2023PA004674.
549 <https://doi.org/10.1029/2023PA004674>

550 Rae, J. W. B., Foster, G. L., Schmidt, D. N., & Elliott, T. (2011). Boron isotopes and B/Ca in benthic
551 foraminifera: Proxies for the deep ocean carbonate system. *Earth and Planetary Science Letters*,
552 302(3–4). <https://doi.org/10.1016/j.epsl.2010.12.034>

553 Rosenthal, Y., Field, M. P., & Sherrell, R. M. (1999). Precise determination of element/calcium ratios in
554 calcareous samples using sector field inductively coupled plasma mass spectrometry. *Analytical
555 Chemistry*, 71(15). <https://doi.org/10.1021/ac981410x>

556 Rosenthal, Y., Lear, C. H., Oppo, D. W., & Linsley, B. K. (2006). Temperature and carbonate ion effects
557 on Mg/Ca and Sr/Ca ratios in benthic foraminifera: Aragonitic species *Hoeglundina elegans*.
558 *Paleoceanography*, 21(1). <https://doi.org/10.1029/2005PA001158>

559 Stewart, J. A., Robinson, L. F., Day, R. D., Strawson, I., Burke, A., Rae, J. W. B., et al. (2020). Refining
560 trace metal temperature proxies in cold-water scleractinian and stylasterid corals. *Earth and*
561 *Planetary Science Letters*, 545. <https://doi.org/10.1016/j.epsl.2020.116412>

562 Stewart, J. A., Christopher, S. J., Kucklick, J. R., Bordier, L., Chalk, T. B., Dapoigny, A., et al. (2021).
563 NIST RM 8301 Boron Isotopes in Marine Carbonate (Simulated Coral and Foraminifera Solutions):
564 Inter-laboratory $\delta^{11}\text{B}$ and Trace Element Ratio Value Assignment. *Geostandards and Geoanalytical*
565 *Research*, 45(1). <https://doi.org/10.1111/ggr.12363>

566 Stirpe, C. R., Allen, K. A., Sikes, E. L., Zhou, X., Rosenthal, Y., Cruz-Uribe, A. M., & Brooks, H. L.
567 (2021). The Mg/Ca proxy for temperature: A *Uvigerina* core-top study in the Southwest Pacific.
568 *Geochimica et Cosmochimica Acta*, 309. <https://doi.org/10.1016/j.gca.2021.06.015>

569 Tisserand, A. A., Dokken, T. M., Waelbroeck, C., Gherardi, J. M., Scao, V., Fontanier, C., & Jorissen, F.
570 (2013). Refining benthic foraminiferal Mg/Ca-temperature calibrations using core-tops from the
571 western tropical Atlantic: Implication for paleotemperature estimation. *Geochemistry, Geophysics,*
572 *Geosystems*, 14(4). <https://doi.org/10.1002/ggge.20043>

573 U.S. EPA. (2014). Method 6020B (SW-846): Inductively Coupled Plasma-Mass Spectrometry. Revision
574 2. Washington, DC. <https://www.epa.gov/esam/epa-method-6020b-sw-846-inductively-coupled-plasma-mass-spectrometry>

575 Umling, N. E., Oppo, D. W., Chen, P., Yu, J., Liu, Z., Yan, M., et al. (2019). Atlantic Circulation and Ice
576 Sheet Influences on Upper South Atlantic Temperatures During the Last Deglaciation.
577 *Paleoceanography and Paleoclimatology*, 34(6). <https://doi.org/10.1029/2019PA003558>

578 Valley, S. G., Lynch-Stieglitz, J., & Marchitto, T. M. (2019). Intermediate water circulation changes in the
579 Florida Straits from a 35 ka record of Mg/Li-derived temperature and Cd/Ca-derived seawater
580 cadmium. *Earth and Planetary Science Letters*, 523, 115692.
581 <https://doi.org/10.1016/j.epsl.2019.06.032>

582 Yu, J., & Elderfield, H. (2007). Benthic foraminiferal B/Ca ratios reflect deep water carbonate saturation
583 state. *Earth and Planetary Science Letters*, 258(1–2). <https://doi.org/10.1016/j.epsl.2007.03.025>

584 Yu, J., Day, J., Greaves, M., & Elderfield, H. (2005). Determination of multiple element/calcium ratios in
585 foraminiferal calcite by quadrupole ICP-MS. *Geochemistry, Geophysics, Geosystems*, 6(8).
586 <https://doi.org/10.1029/2005GC000964>

587 Yu, J., Elderfield, H., Jin, Z., Tomascak, P., & Rohling, E. J. (2014). Controls on Sr/Ca in benthic
588 foraminifera and implications for seawater Sr/Ca during the late Pleistocene. *Quaternary Science*
589 *Reviews*, 98. <https://doi.org/10.1016/j.quascirev.2014.05.018>

590

591

592

Figure 1.

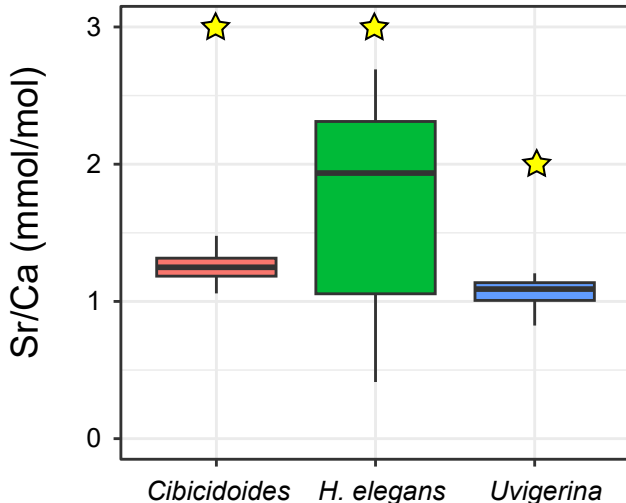
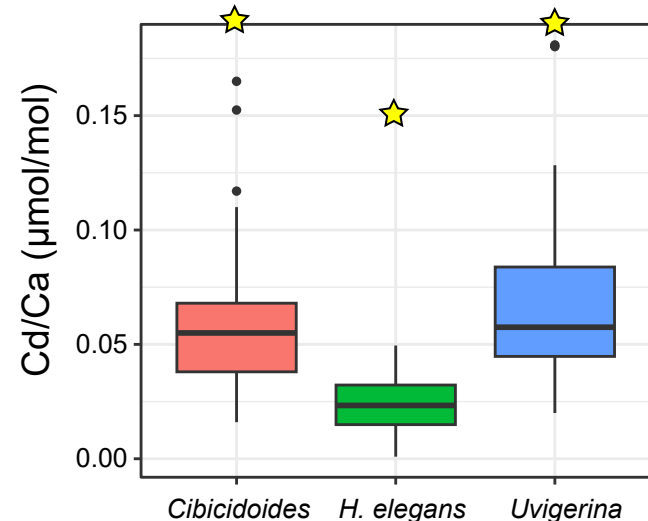
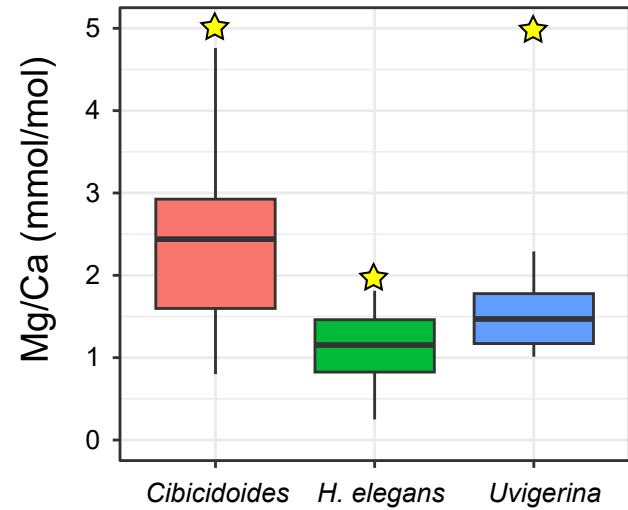
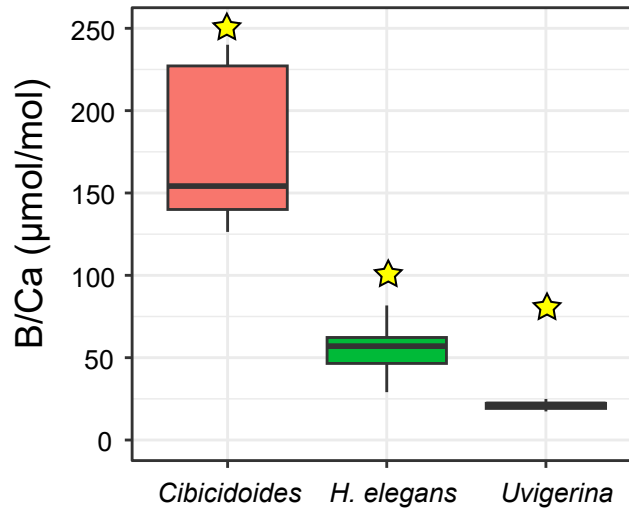
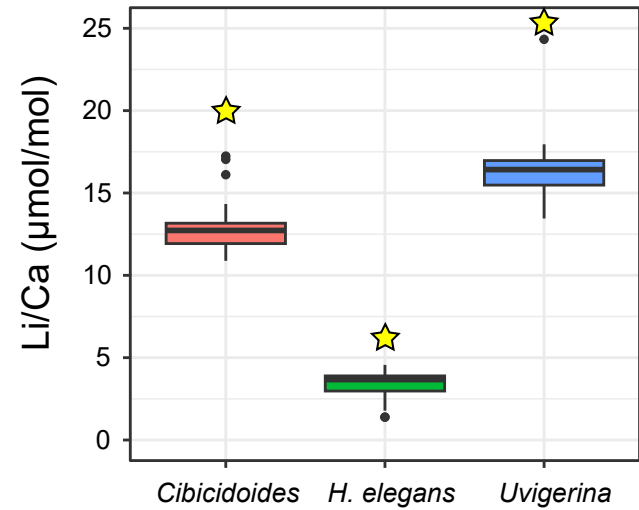
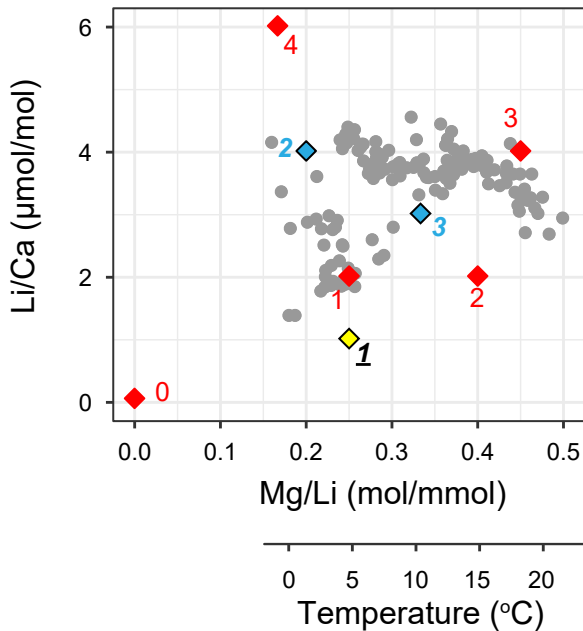
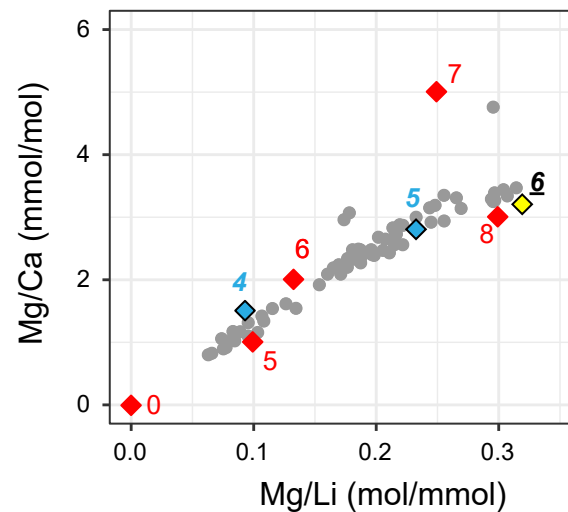
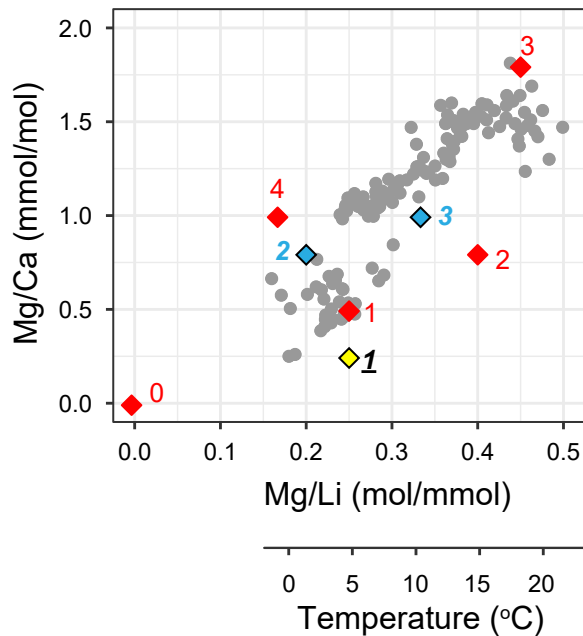
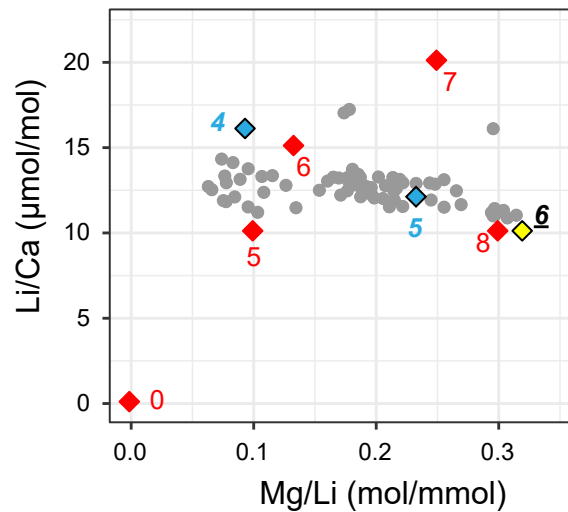


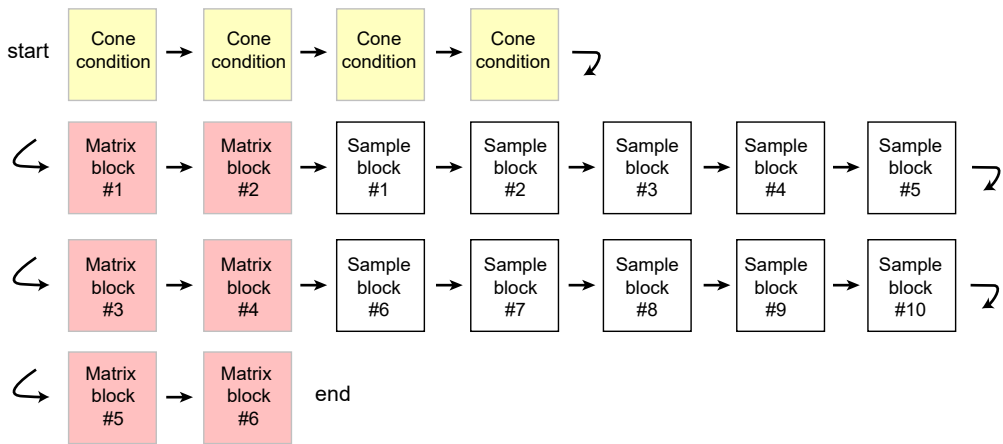
Figure 2.

H. elegans*Cibicidoides*

- Core-top forams
- ◆ Calibration stds (GLU)
- ◆ Matrix stds (AFS)
- ◆ Consistency stds (AFS)

Figure 3.

A) Session structure



B) Cone conditioning

Blank (2% HNO3)
AFS3_100ppmCa
Blank (2% HNO3)
AFS3_100ppmCa
AFS3_100ppmCa
AFS3_100ppmCa
AFS3_100ppmCa
Blank (2% HNO3)
AFS3_100ppmCa

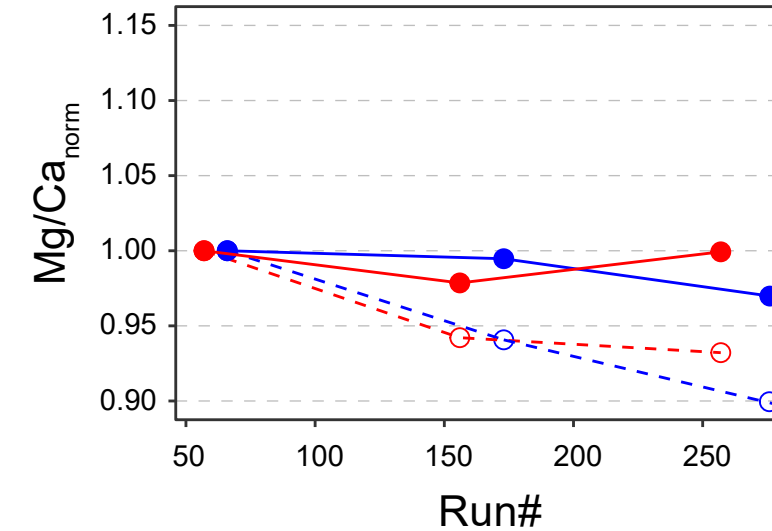
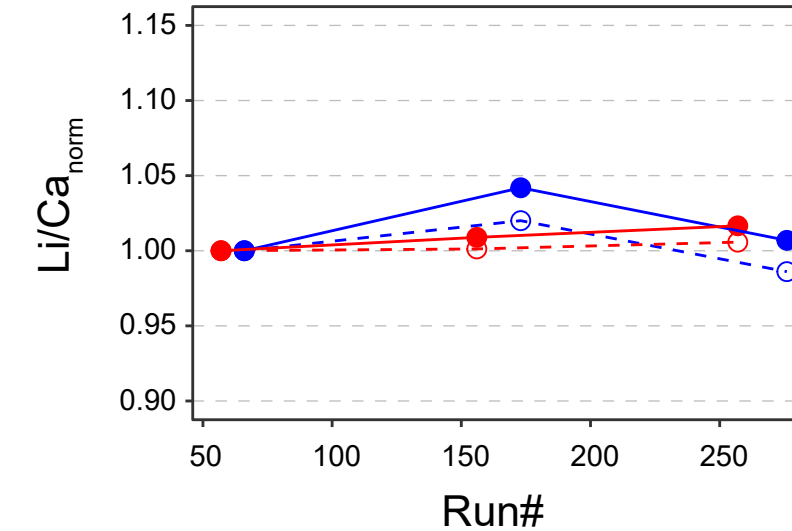
C) Matrix block

Blank (2% HNO3)
GLU0_Std
Matrix 1
Matrix 2
GLU1_Std
Matrix 3
Matrix 4
GLU2_Std
Matrix 5
Matrix 6
GLU3_Std
Matrix 7
Matrix 8
GLU4_Std

D) Sample block

Blank (2% HNO3)
GLU0_Std
Sample 1
Sample 2
GLU1_Std
Sample 3
Sample 4
GLU2_Std
Sample 5
Sample 6
GLU3_Std
Sample 7
Sample 8
GLU4_Std

Figure 4.



Matrix std: AFS2 at 100 ppm Ca
Matrix std: AFS3 at 100 ppm Ca

Before std correction (normalized CPS/CPS data)

○ ○ - - - - -

After std correction (normalized molar ratio data)

● ● — — — — —

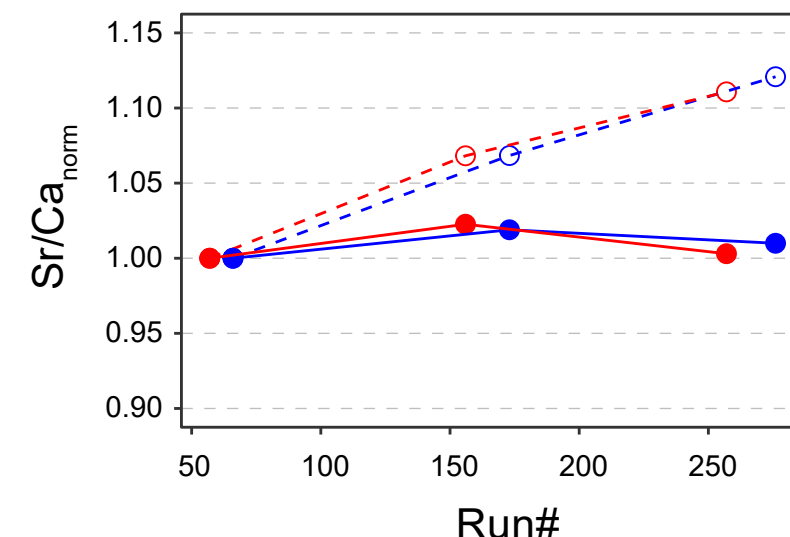
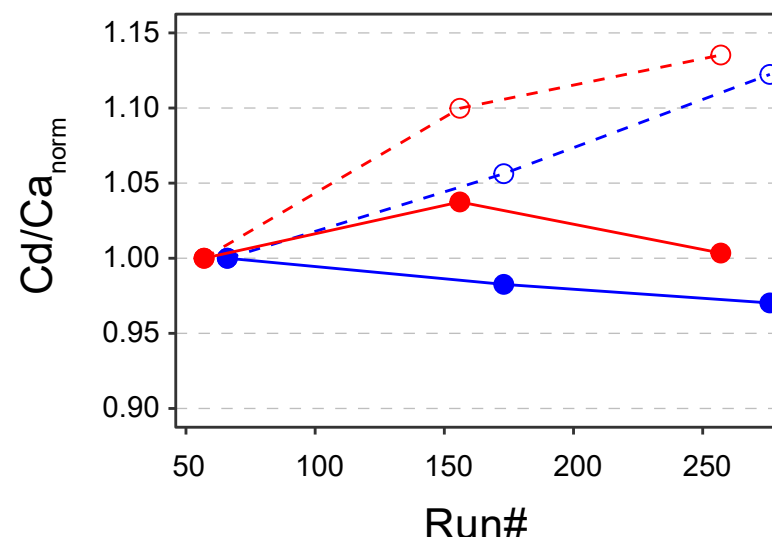
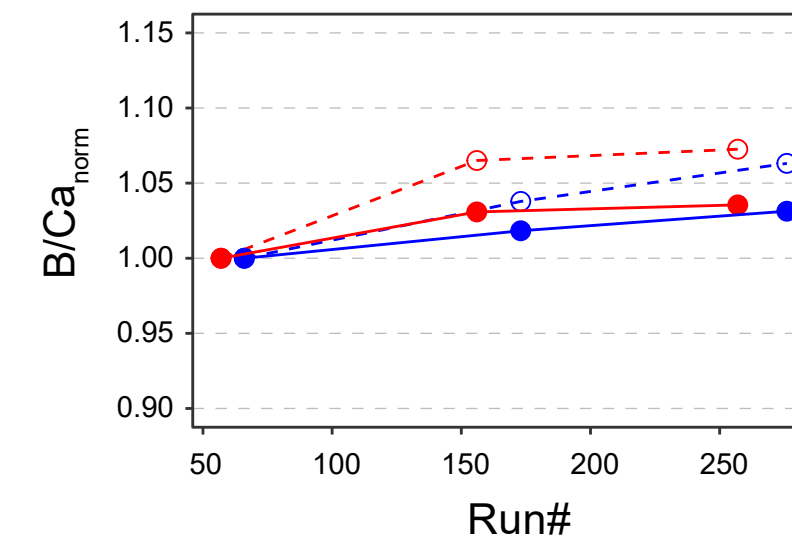
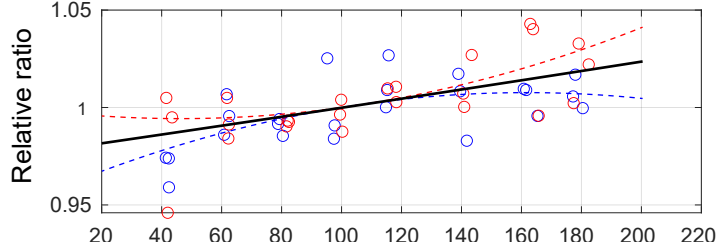
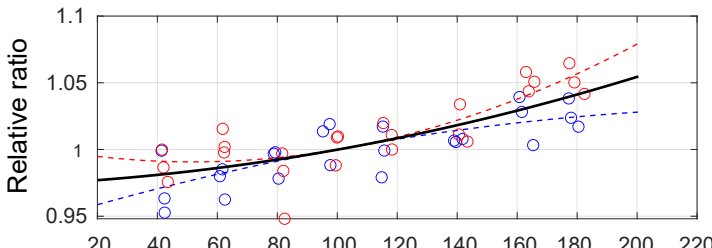


Figure 5.

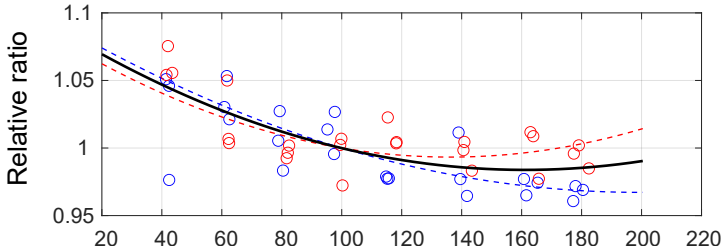
Li/Ca



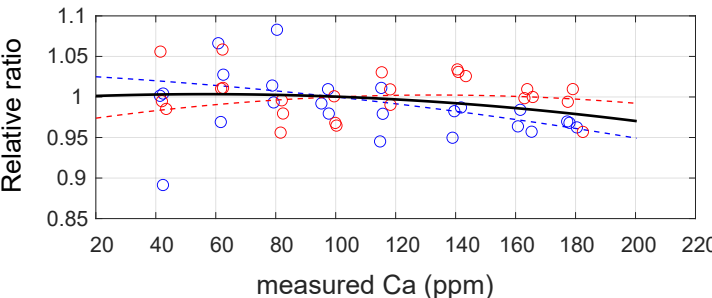
Mg/Ca



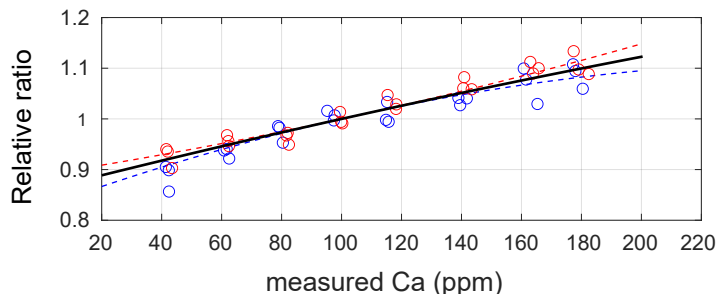
B/Ca



Cd/Ca



Sr/Ca



○ AFS2
○ AFS3

Figure 6.

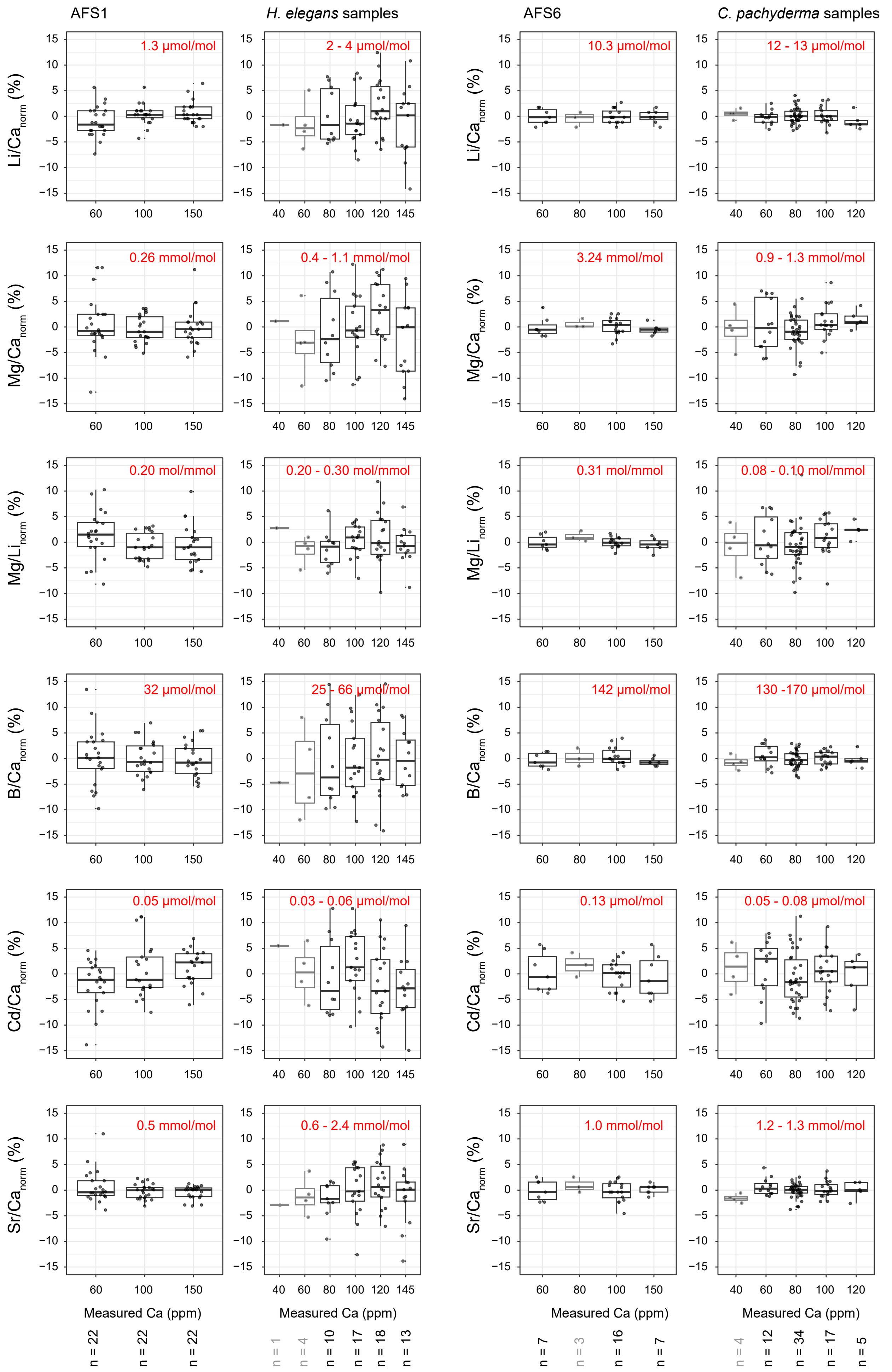


Figure 7.

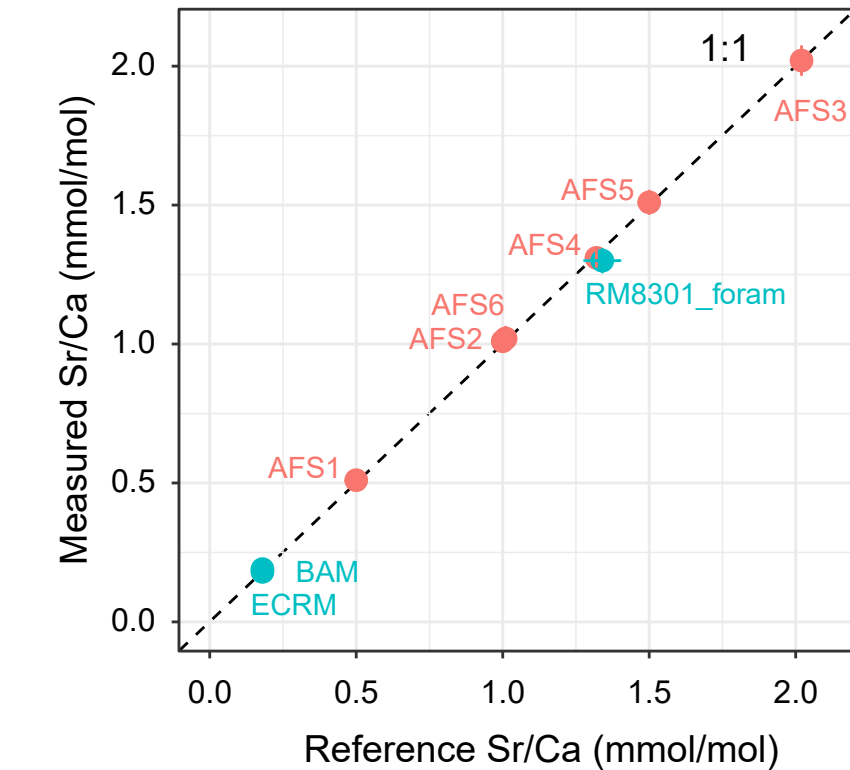
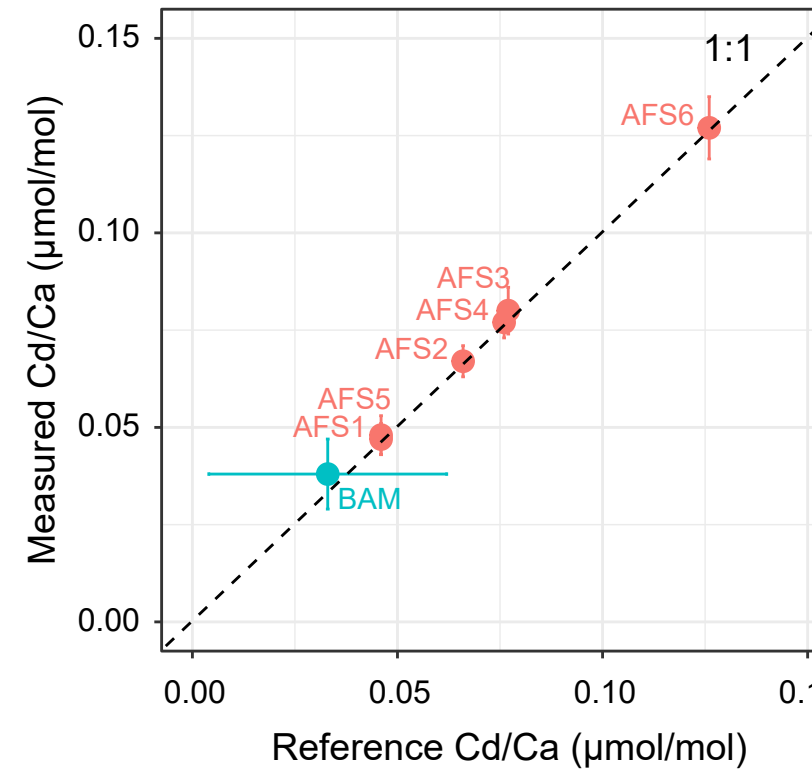
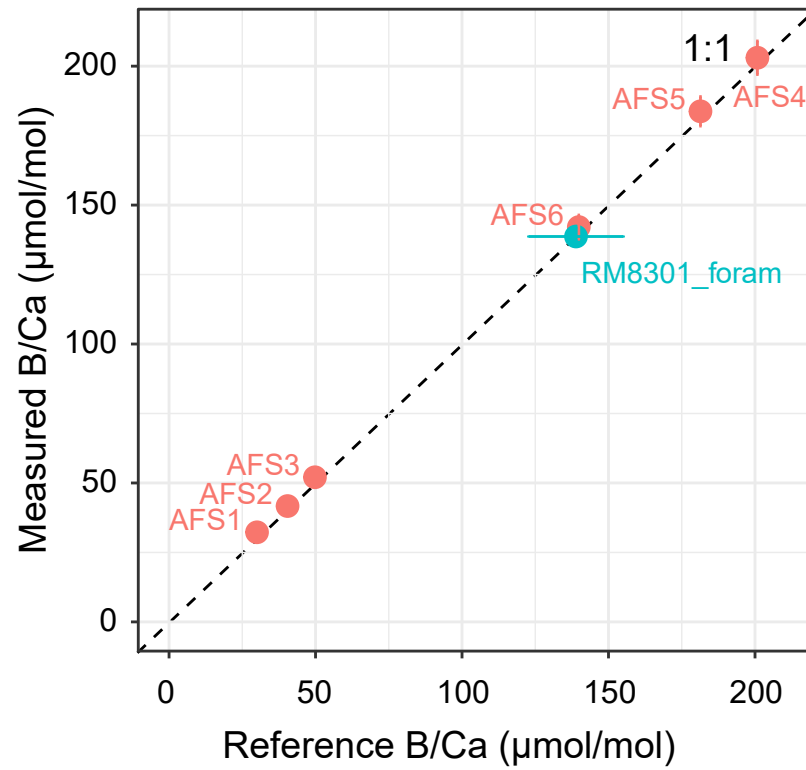
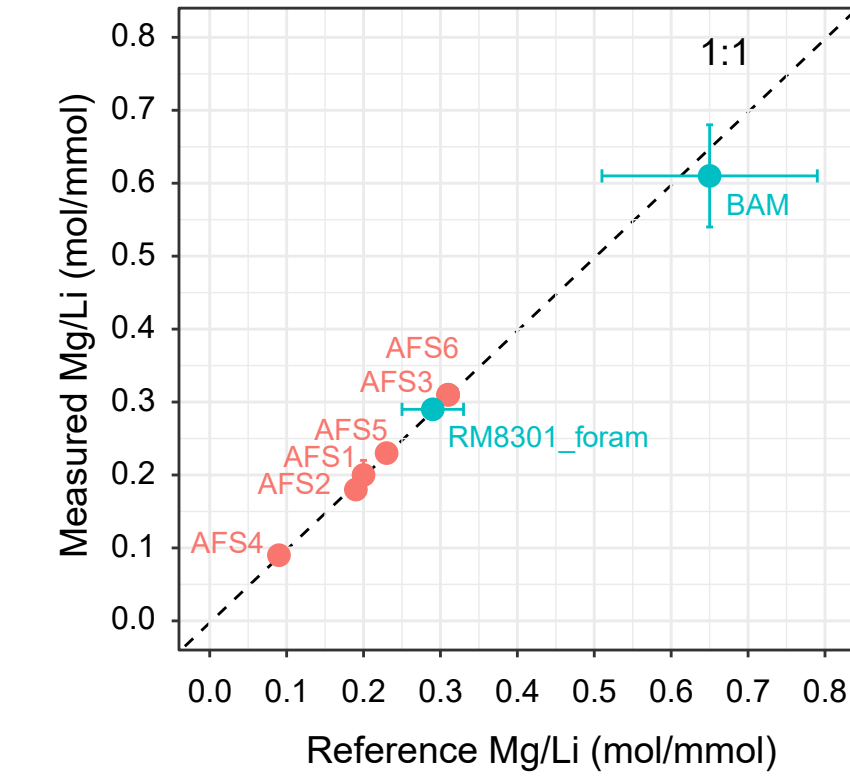
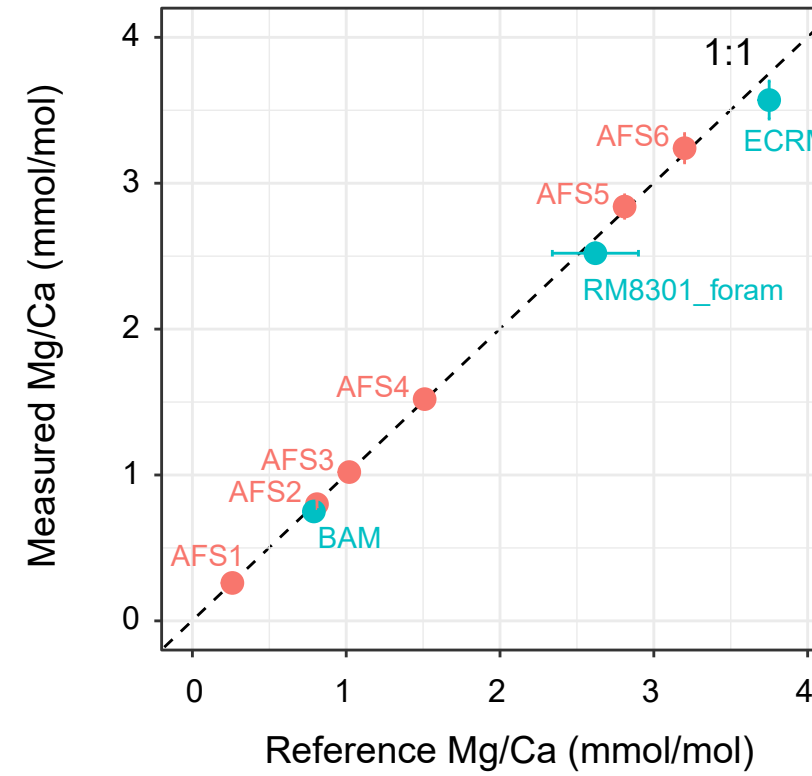
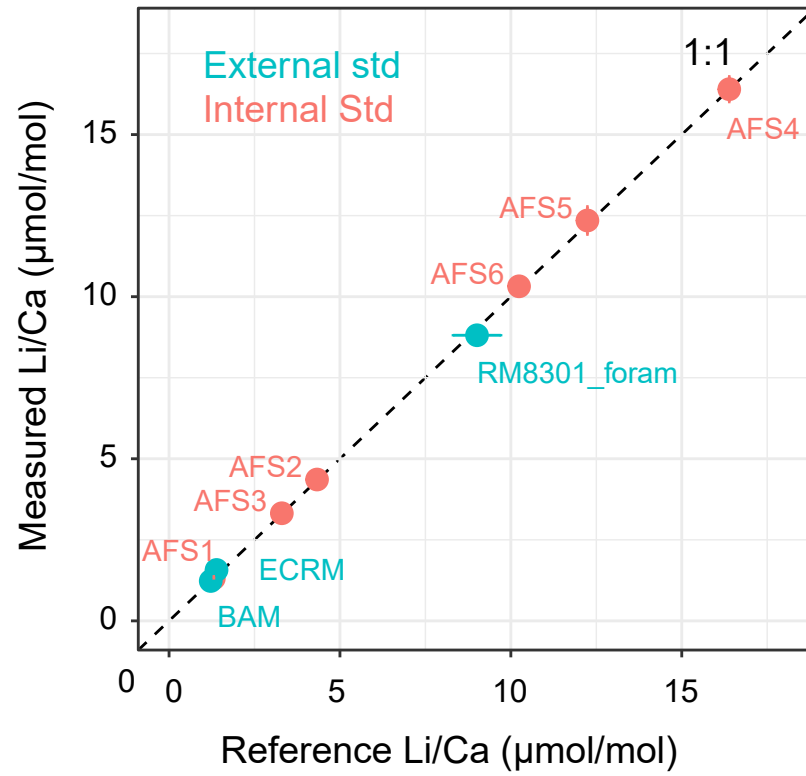
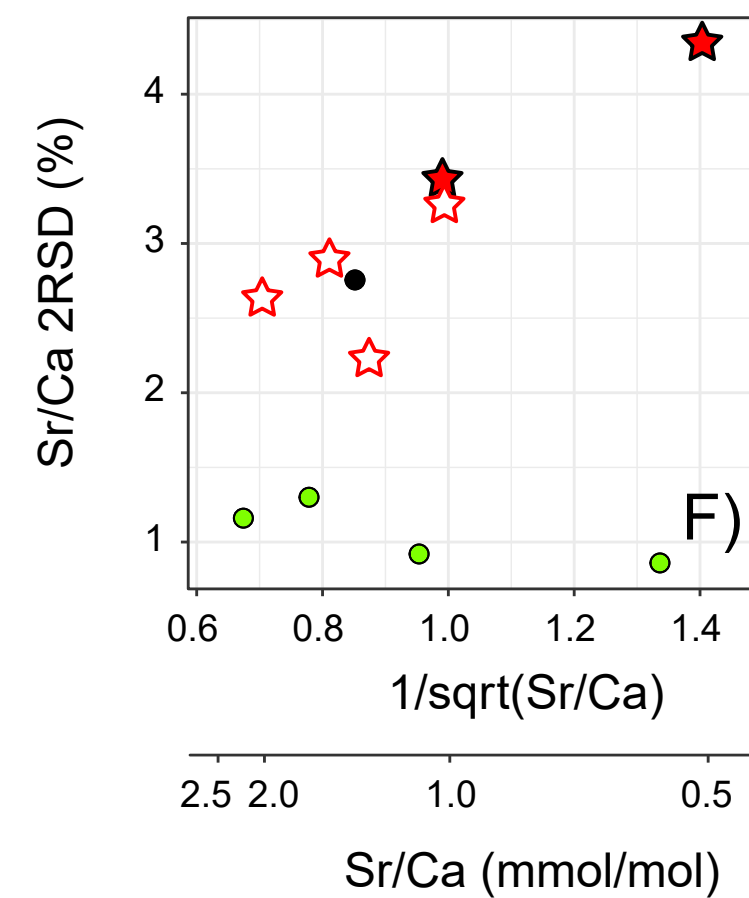
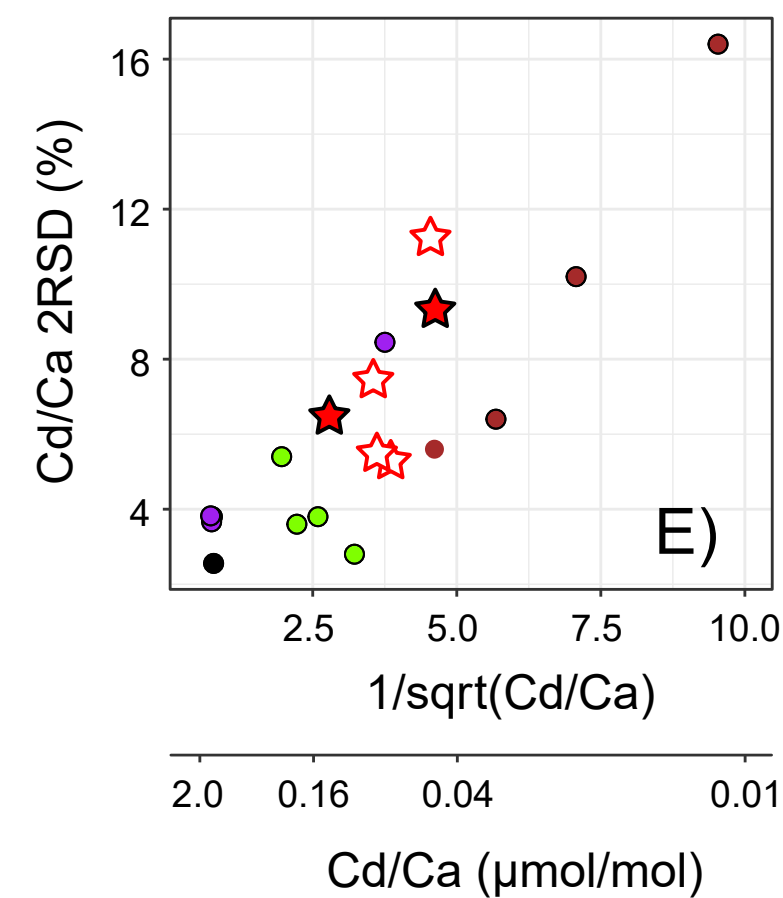
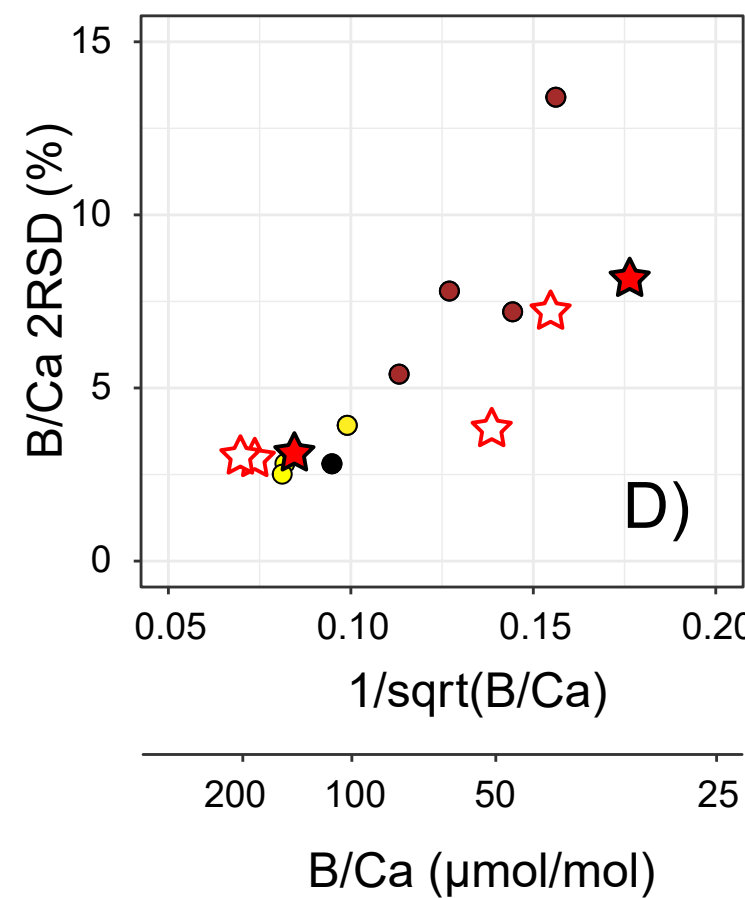
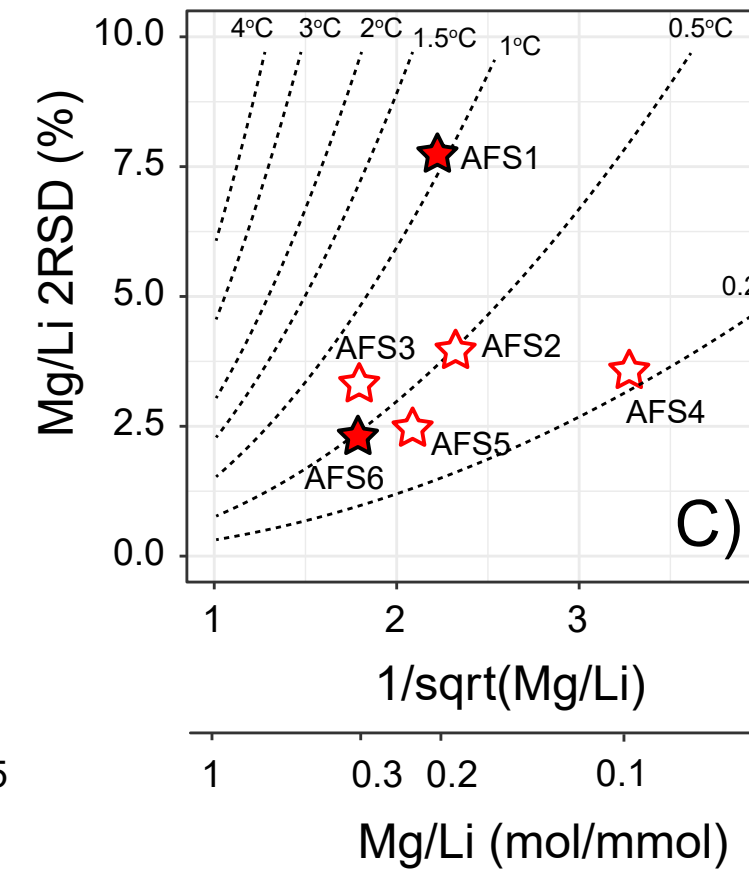
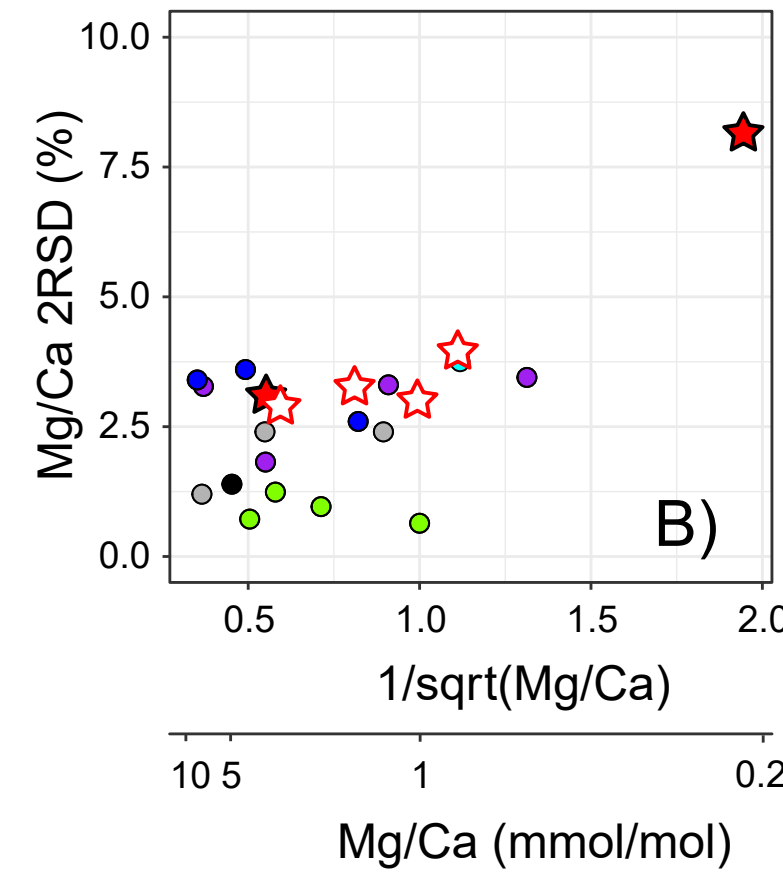
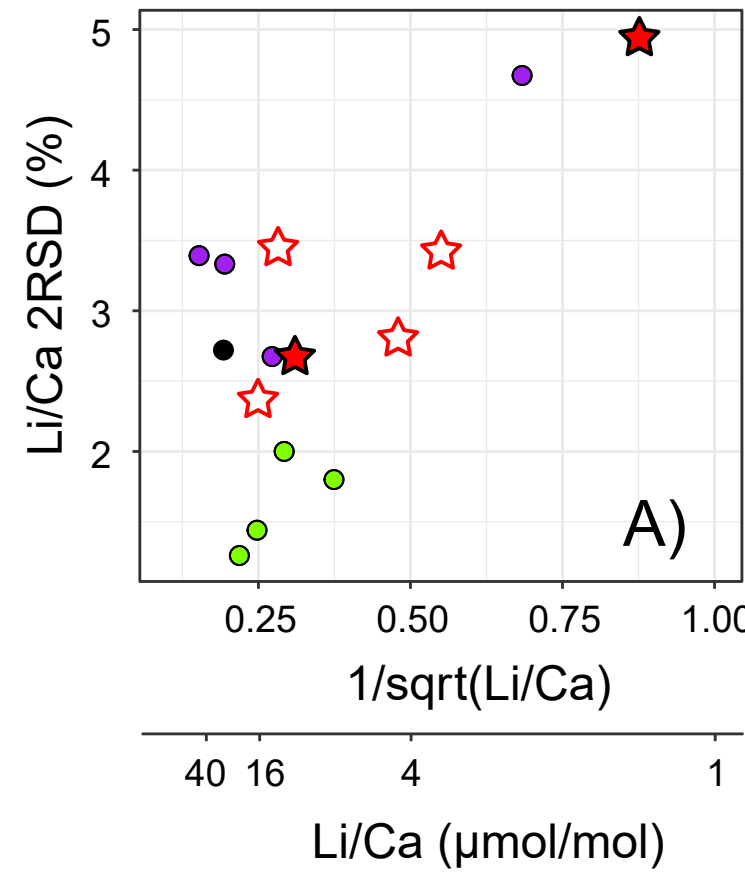


Figure 8.



WHOI iCAP-Q

- ★ this study, internal std @ varying Ca
- ★ this study, internal std @ 100 ppm Ca
- Umling et al. 2019. internal std @ 60 ppm Ca

Other labs

- Element XR, Oppo et al. 2023
- iCAP, Dai et al. 2023
- Perkin-Elmer, Yu et al. 2005
- Element 2, Marchitto 2006
- iCAP, Ford et al. 2016
- Element XR, Ford et al. 2016